Best Available Copy

INVESTIGATION OF FEASIBILITY OF UTILIZING AVAILABLE HEAT-RESISTANT MATERIALS FOR HYPERSONIC LEADING EDGE APPLICATIONS

VOLUME IV

[illegible]

[illegible]

J.J. LANG

[illegible] FOUNDATION

[illegible]

[illegible] LITTLE, INC.

JUL 1960

[illegible]

NOTICES

When Government drawings, specifications, or other data are used for any purpose other than in connection with a definitely related Government procurement operation, the United States Government thereby incurs no responsibility nor any obligation whatsoever; and the fact that the Government may have formulated, furnished, or in any way supplied the said drawings, specifications, or other data, is not be regarded by implication or otherwise as in any manner licensing the holder or any other person or corporation, or conveying any rights or permission to manufacture, use, or sell any patented invention that may in any way be related thereto.

- - - - -

Qualified requesters may obtain copies of this report from the Armed Services Technical Information Agency (ASTIA).

This report has been released to the Office of Technical Services, Department of Commerce, Washington 25, D. C., for sale to the general public.

Copies of WADC Technical Notes and Technical Reports should not be returned to Wright Air Development Center unless return is specifically required by special security considerations, contractual obligations, or notice on a specific document.

WADC TECHNICAL REPORT 59-744
Volume IV

INVESTIGATION OF FEASIBILITY OF UTILIZING AVAILABLE HEAT RESISTANT MATERIALS FOR HYPERSONIC LEADING EDGE APPLICATIONS

VOLUME IV

Thermal Properties of Molybdenum Alloy and Graphite

I. B. Fieldhouse
J. I. Lang
Armour Research Foundation

H. H. Blau, Jr.
Arthur D. Little, Inc.

July 1960

Materials Laboratory
Contract No. AF 33(616)-6034
Project No. 7350

Aircraft Laboratory
Project No. 1368

Wright Air Development Center
Air Research and Development Command
United States Air Force
Wright-Patterson Air Force Base, Ohio

FOREWORD

This work was conducted by Bell Aircraft Corporation under USAF Contract No. AF 33(616)-6034. Mr. Frank M. Anthony acted as project engineer. This contract was initiated under Materials Laboratory Project No. 7350 "Ceramic and Cermet Materials", Task No. 73500 "Ceramic and Cermet Materials Development", and Aircraft Laboratory Project No. 1368 "Construction Techniques and Application of New Materials", Task No. 13719 "Re-entry Structures". This work was administered under the combined direction of the Materials Laboratory and the Aircraft Laboratory, Directorate of Laboratories, Wright Air Development Center, with Mr. J. J. Krochmal and Lt. J. Latva acting as Project Engineers for the Materials Laboratory, and Mr. C. J. Cosenza acting as Project Engineer for the Aircraft Laboratory.

This report covers work conducted from July 1958 to July 1960.

This particular report, Volume IV, is one of a series which, when combined, constitute the final technical report on this contract. In total, this technical report contains

Volume I	Summary
Volume II	Analytical Methods and Design Studies
Volume III	Screening Test Results and Selection of Materials
Volume IV	Thermal Properties of Molybdenum Alloy and Graphite
Volume V	Mechanical Properties of Bare and Coated Molybdenum Alloy
Volume VI	Determination and Design Application of Mechanical Properties of Bare and Coated Graphite
Volume VII	Oxidation Resistance of Bare and Coated Molybdenum Alloy and Graphite
Volume VIII	Tests of Molybdenum and Graphite Leading Edge Components
Volume IX	Applicability to Future Weapon Systems

Volumes I through VIII are unclassified, while Volume IX is classified Secret.

ABSTRACT

The purpose of this contract was to investigate the feasibility of utilizing available heat resistant materials in the fabrication of leading edges for hypersonic boost-glide vehicles. This particular volume presents the results of measurements of the thermal conductivity, specific heat, linear thermal expansion, and emittance of a 0.5% titanium alloy of molybdenum, and of siliconized ATJ graphite as a function of temperature. Emittance measurements were made on coated and uncoated materials.

PUBLICATION REVIEW

This report has been reviewed and approved.

FOR THE COMMANDER:

W. G. RAMKE
Chief, Ceramics and Graphite Branch
Metals and Ceramics Laboratory
Materials Central

TABLE OF CONTENTS

LIST OF TABLES

LIST OF ILLUSTRATIONS

LIST OF ILLUSTRATIONS (Continued)

I. INTRODUCTION

The scope of this study encompassed the many considerations required for the investigation of the feasibility of using available heat resistant materials for the leading edges of hypersonic vehicles. The boost-glide vehicle concept formed the basis for this work with the flight parameter W/SC_L ranging from 100 to 400. Manned and unmanned, reusable and expendable flight vehicles were considered with emphasis being placed on manned, unmanned, reusable systems. For purposes of this study maximum temperatures were to range from 2500°F to 3000°F. Ablation and cooling techniques were excluded.

The objective of the study was to determine the feasibility of employing available materials for the desired application. This goal was achieved by describing available materials to the degree required for design purposes, by establishing suitable design methods, by considering the peculiarities of materials in design, by indicating approximate operating temperatures and flight trajectories possible when various existing materials were used for leading edges, and finally, by actual testing of two typical leading edge designs. Many secondary benefits resulted from this study, including a better mutual understanding of the problems confronting material suppliers and airframe designers, a definition of the shortcomings of existing materials for this application which should form a foundation for future material development, an advancement in design technology for brittle materials used for structural applications, and a definition of critical parameters which would require laboratory simulation prior to actual usage of leading edge elements.

This study was conducted in four essentially concurrent phases; they involved design, materials evaluation, fabrication and component testing. The design phase investigated trajectories for hypersonic vehicles to establish a range of typical flight and environmental conditions. Design criteria required to insure structural integrity of heat resistant leading edges were investigated and tentatively established. Methods for the determination of temperatures, temperature gradients and thermal stresses were established and adapted to automatic computing equipment. The effects of leading edge geometry, both external and internal, on temperatures, temperature gradients and thermal stresses were studied as well as attachment details for metallic and non-metallic leading edges and the effects of various restraints upon thermal stresses. The design phase culminated with the design of two leading edges, one using metallic and the other using non-metallic material; both types were tested.

Note: Manuscript copy released by the authors July 1960 for publication as a WADC Technical Report

The materials evaluation phase began with a literature review to obtain known physical and mechanical characteristics of refractory metals and non-metals supplemented by contacts with material suppliers. A preliminary experimental evaluation of a number of promising metals, non-metals and coatings was conducted in order to supply data not found in the literature and to provide consistent sets of material property data for use in making meaningful comparisons. Based upon the results of the preliminary evaluations and upon fabrication considerations the single most promising metal, 0.5% titanium alloy of molybdenum, the single most promising non-metal, siliconized ATJ graphite, and the two most promising coatings were evaluated in detail to provide the material property data required for design purposes. The detailed evaluation of the selected non-metallic material included an investigation to establish relationships required for the design of components using brittle materials.

The fabrication phase included the preparation of most of the test specimens as well as the production of the final leading edge designs. Test specimens were produced by techniques and process procedures similar to those expected to be required in the manufacture of final leading edge components. Restriction of the manufacturing process in such a manner may preclude attainment of the maximum material properties which could be achieved by employing the optimum fabrication techniques for small test bars. It did, however, provide a means of correlating test results and analytical predictions, since the material properties of the components should be approximately the same as those determined from the test specimens. For example, ceramic materials generally exhibit higher thermal conductivity and higher strength when fabricating by hot pressing than when fabricated from slip casting. While simple test bars can be made by hot pressing it may be necessary to fabricate more complex shapes by slip casting and test results on hot pressed bars are of little or no value in defining the characteristics of the slip case component.

The component testing phase included several items of study. Typical attachments for brittle components were tested to aid in the selection of suitable designs. Finally a metallic leading edge design and a non-metallic design were tested under partially simulated conditions.

In order to achieve maximum efficiency, of both time and cost, and to integrate more closely the materials and design problems, extensive subcontracting was employed during this study. All specimen and component fabrication was done by subcontractors having extensive experience with the materials and fabrication procedures required. Existing testing capabilities of organizations throughout the country were utilized to the fullest possible extent.

This particular volume presents the results of measurements which were made to determine thermal conductivity, specific heat, linear thermal expansion, and emittance of a 0.5% titanium alloy of molybdenum and a siliconized ATJ graphite as a function of temperature. Emittance measurements were made on coated and uncoated materials.

II. THERMAL CONDUCTIVITY

Description of Equipment

The thermal conductivity of the selected materials was determined by using the radial heat flow method developed by R. W. Powell. This method consists of measuring, during steady state, the radial flow and radial temperature drop in a vertical stack of disks composed of the material whose thermal conductivity is to be measured. The equipment was calibrated by determining the thermal conductivity of Armco iron. The results agreed closely with accepted values.

The radial heat flow method developed by R. W. Powell[1] was used to measure the thermal conductivity of the test specimens. With this method, the radial heat flow and radial temperature drop was measured in a vertical stack of disks composed of the material whose thermal conductivity was to be determined. More specifically, the disks were in the form of annular rings and radial heat flow through the disks was supplied by an electric heater centered in the axial hole of the stacked disks. In order to obtain high temperatures as well as to control the temperature gradient in the test specimens, the column of stacked disks was placed in an electrically heated furnace in which a helium atmosphere was maintained. The radial heat flow through a section of the stacked disks three inches long, 1.5 inches above and below the vertical center of the column, was derived from measurement of the current and voltage-drop along a three-inch length of the axial heater adjacent to the test section. The temperature gradient was measured by means of thermocouples inserted in small vertical holes, one near the axial hole containing the heater and the other near the outer edge of the disks. The thermal conductivity of the disk material was calculated under steady state conditions from the power input, the radial distance of the inner and outer thermocouples from the axis of the disks, and the temperature difference between these holes. A section through the apparatus which was used is shown in Figure 1.

Test Procedure

Each set of test specimens contained 15 disks; three of which were one inch thick and 12 were 1/2 inch thick. The three one-inch thick disks were located in the center of the stack, called the test section, and six 1/2 inch thick disks were located at each end, and called the guard sections.

---

1. Powell, R. W. "Proceedings of the Physical Society". London, Vol. 46, pp 659-674, 1934.

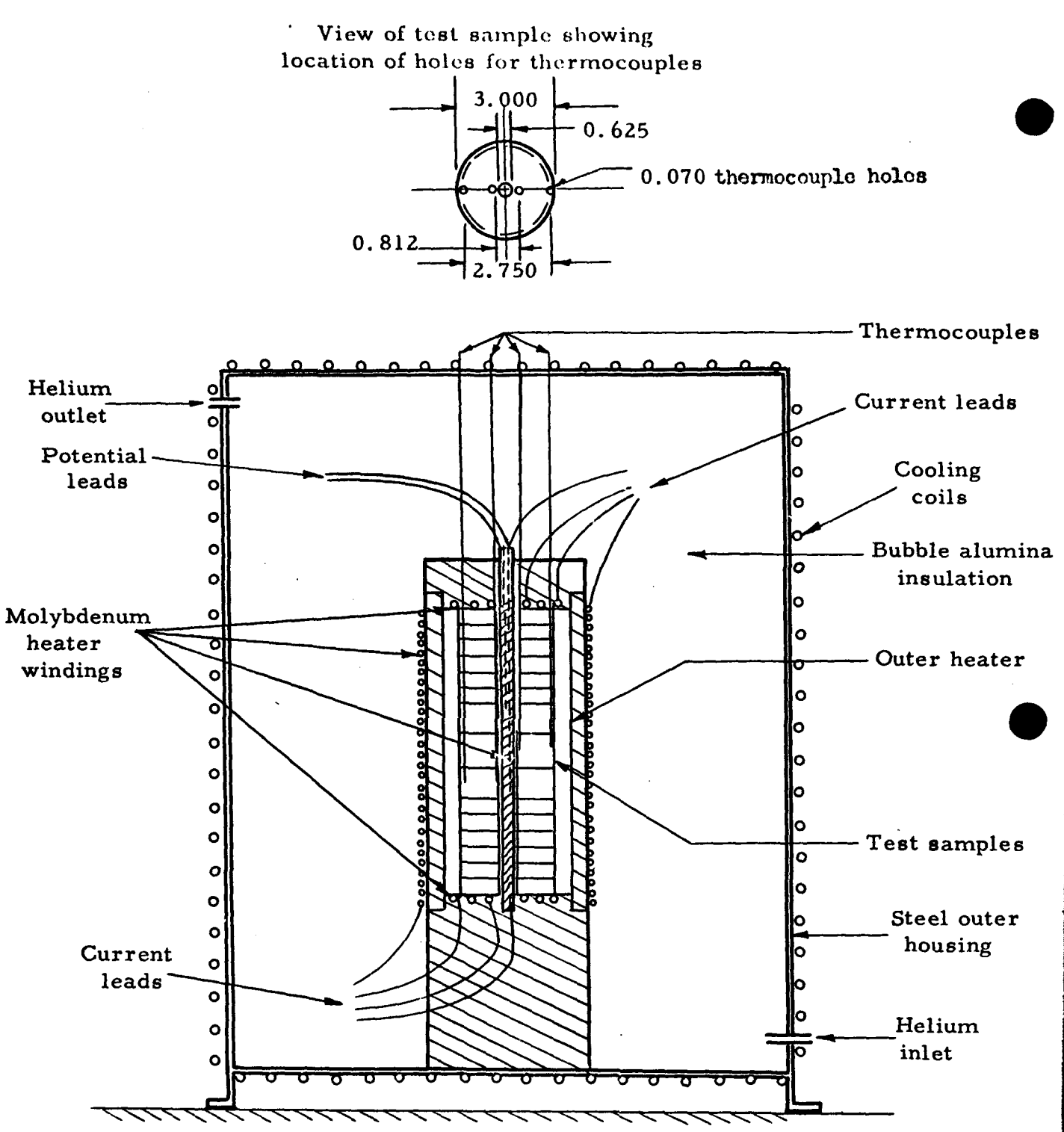

Figure 1. GENERAL LAYOUT OF THERMAL CONDUCTIVITY STACKED DISK APPARATUS

As shown in Figure 1, four holes were located in each disk to permit insertion of thermocouples. Platinum, platinum - 10% - rhodium thermocouples protected by pure alumina tubing were used for measuring temperatures. The thermocouples were connected so that the temperature difference as well as the temperature level could be measured. With respect to the thermocouples, the accuracy of the final results depends primarily on the calibration accuracy of each couple relative to the others, and only reasonable accuracy is required as to absolute temperature measurement. The couples were calibrated relative to each other and checked within 0.1°F. The thermocouples were moved up and down so that a temperature traverse along the length of the samples would be made. It was necessary to measure the axial temperature distribution in order to determine if any heat was flowing in the axial direction. Axial heat flow would introduce an error since it was assumed in the calculations that the heat flow in the three center disks was in the radial direction only. One reason for using disks rather than a single cylinder was that the poor thermal contact between disks offers considerable resistance to axial heat flow. In order to further insure that axial heat flow would not occur, molybdenum wound heaters were placed at both ends of the test specimens.

In performing the experimental measurements, the axial temperature gradient between the vertical center and the ends of the stack was less than 1°F. The radial temperature difference between the inner and outer thermocouples was maintained at 25°F over the entire mean temperature range at which the measurements were made. This radial temperature difference was identical on both sides of the axis.

The radial heat flow through the test specimens was accomplished by a molybdenum coil wound on a ceramic core and centered in the axial hole of the atacked disks. As shown in Figure 1, the stacked disks were placed in a ceramic tube which had a molybdenum coil wound around the outer surface. The outer heater provided the energy needed to raise the temperature of the sample while the inner heater provided a means of varying the temperature drop through the sample. The three one-inch thick samples located in the center of the stack were considered as the test section, and the current and voltage-drop in the inner heater was measured over this three-inch length. The outer heater was surrounded by bubble alumina insulation and a water-cooled steel housing. The apparatus was purged with helium to provide an inert atmosphere.

The thermal conductivity was calculated by the following equation:

$$k = \frac{Q \ln r_2/r_1}{2\pi L (\Delta t)} \qquad (1)$$

where

k = thermal conductivity, BTU hr^{-1} ft^{-1} $^oF^{-1}$

Q = radial heat flow, BTU hr^{-1}

L = length of test section, ft

r_1 = radial distance from axis to inner thermocouple, ft

r_2 = radial distance from axis to outer thermocouple, ft

Δt = temperature drop over the radial distance between thermocouples, ^{o}F

Experimental Accuracy

Preliminary tests were made using Armco iron test specimens in order to confirm the accuracy of the apparatus. The results of these experiments are given in Table I. These results compare quite well with the results obtained by Powell[2] who felt that the error in his measurements was less than 2%.

Errors in measurement may result from misalignment of the inner and outer heaters, variation in the resistance of the inner heater wire, location of the thermocouples, etc. Because of the close agreement with Powell's data on Armco iron and the small spread in experimental data, it is felt that the accuracy of the ARF results is within 5%.

Test Results

The experimental test results are shown in Tables II, III and IV, and in Figures 2, 3 and 4.

---

2. Powell, R. W. "Proceedings of the Physical Society". London, Vol. 50, p 407, 1938

TABLE I

COMPARISON OF THERMAL CONDUCTIVITY

DATA FOR ARMCO IRON

Mean temperature, °F	Thermal conductivity, BTU/hr ft °F	
	Powell	ARF
212	39.5	39.5
392	35.6	35.6
572	32.0	31.8
752	28.1	28.1
932	25.0	25.0
995	24.0	23.8
1112	22.5	21.8
1292	19.8	18.9
1472	17.2	17.0
1496	16.9	17.0
1615	16.1	17.0
1652	16.0	17.0
1832	16.2	17.0

TABLE II

THERMAL CONDUCTIVITY OF

0.5% TITANIUM ALLOY OF MOLYBDENUM

Mean temperature, °F	Thermal conductivity, BTU/hr ft °F
609.3	68.5
713.6	66.1
769.0	65.9
834.6	64.0
1077.2	59.2
1330.9	53.0
1399.2	50.3
1400.3	50.2
1664.7	46.5
2053.6	37.3
2299.7	30.9
2333.0	27.6
2650.0	23.4
2982.0	17.3
3027.0	15.2

TABLE III

THERMAL CONDUCTIVITY

OF SILICONIZED ATJ GRAPHITE*

Mean temperature, °F	Thermal conductivity, BTU/hr ft °F
639	41.7
646	40.3
1025	34.6
1404	30.7
1820	25.0
2009	22.9
2314	21.0
2620	18.8
2840	17.6
3000	17.0

* Perpendicular to grain orientation

TABLE IV

THERMAL CONDUCTIVITY

OF SILICONIZED ATJ GRAPHITE*

Mean temperature, °F	Thermal conductivity, BTU/hr ft °F
710	53.0
1036	43.2
1325	36.6
1545	32.8
1875	26.5
2021	24.6
2186	20.9
2375	19.9
2520	19.4
2566	19.2
2697	17.9
2856	17.0
3013	16.9

* Parallel to grain orientation

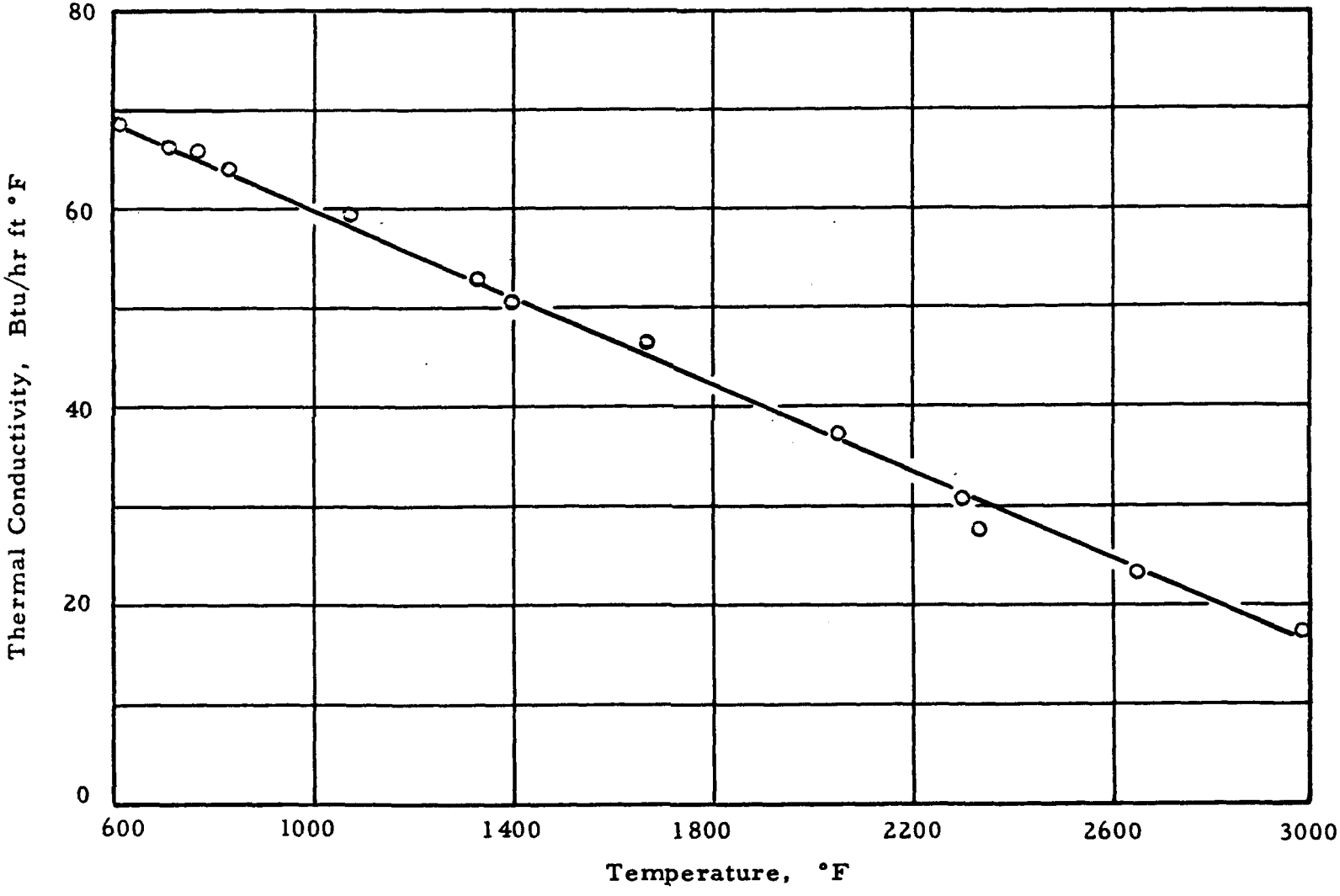

Figure 2. THERMAL CONDUCTIVITY OF 0.5% TITANIUM ALLOY OF MOLYBDENUM

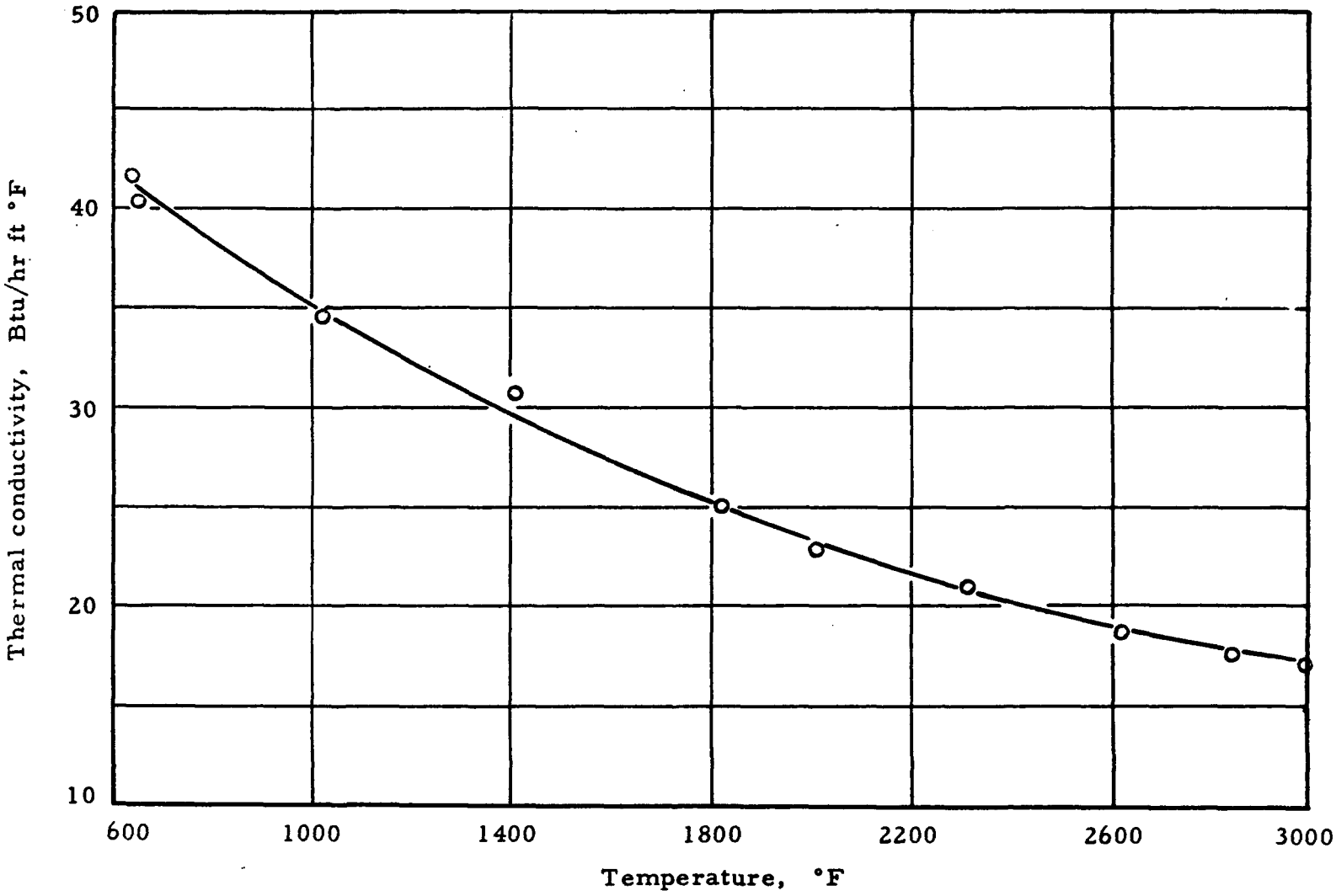

Figure 3. THERMAL CONDUCTIVITY OF SILICONIZED ATJ GRAPHITE

(Perpendicular to Grain Orientation)

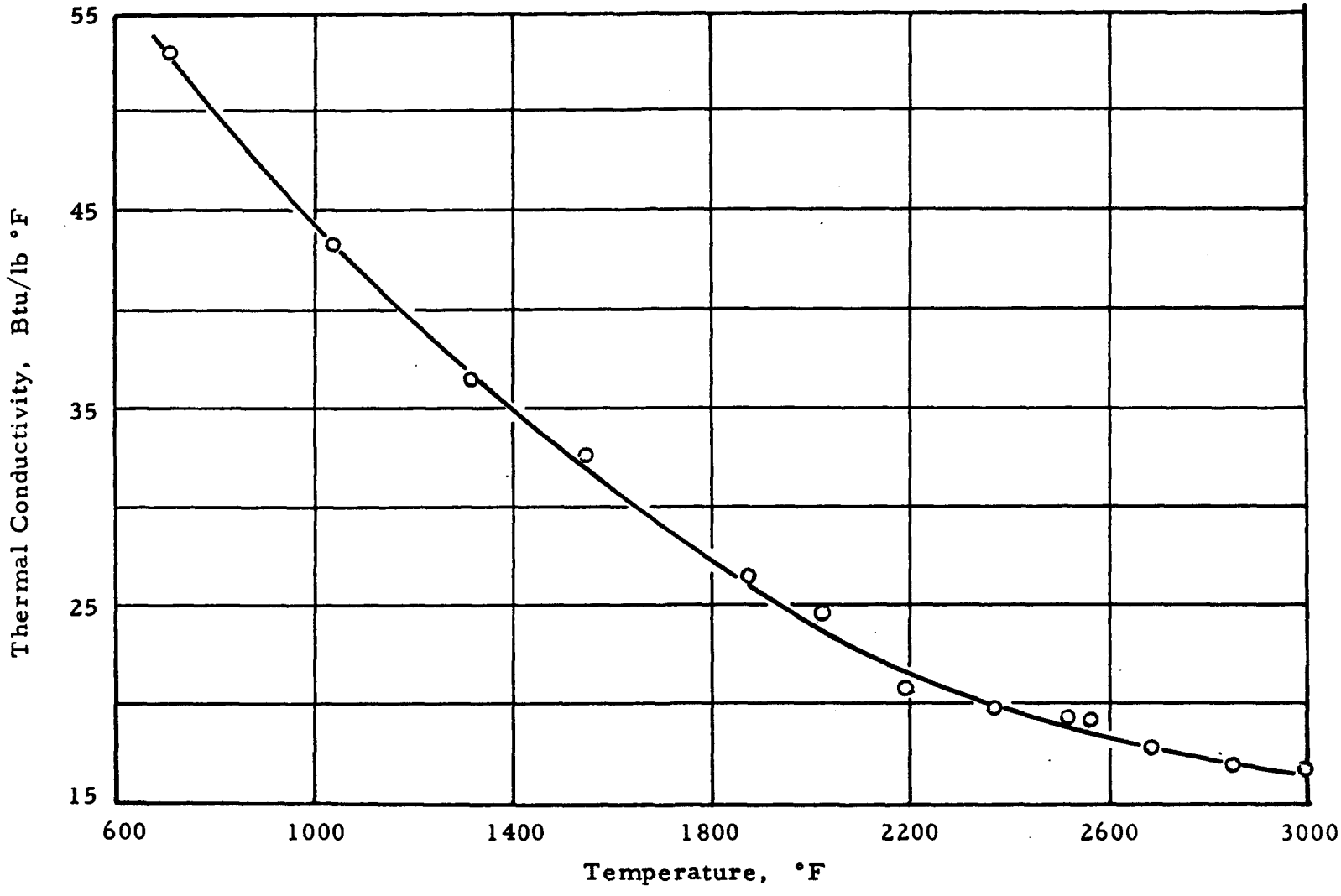

Figure 4. THERMAL CONDUCTIVITY OF SILICONIZED ATJ GRAPHITE

(Parallel to Grain Orientation)

III. SPECIFIC HEAT

Description of Equipment

The apparatus used is shown in Figure 5. The furnace is a vertical tube type purchased from the Harper Electric Company. The interior of the furnace contains an alundum tube, 1-1/2 inches inside diameter, 44 inches in length. The tube length and diameter were specified to assure a uniform temperature region surrounding the sample.

The furnace was heated electrically by a globar tube, exterior to and concentric with the alundum tube. Power input to the globar element was controlled by a 3-step 6-position transformer. An inert atmosphere for the furnace interior was assured by constant purging with helium. Sealing at the top of the tube was attained by a pipe flange; bottom sealing was provided by a globe valve.

The temperature of the furnace at the point where the sample was suspended was measured by two platinum, platinum - 10% - rhodium thermocouples contained in protection tubes and suspended from the furnace top. An axial temperature survey at the in-furnace sample position indicated a temperature gradient of less than $1^{\circ}F$/inch, at a mean furnace temperature of $2500^{\circ}F$.

The furnace tube is connected to the calorimeter by means of a 1-1/2 inch stainless steel pipe. Immediately above the calorimeter, the 1-1/2 inch pipe was reduced by a convergent section to a one inch pipe. The one inch pipe was inserted into the receiver for a length of one inch. The receiver is based on a design described by Ginnings and Corruccini[3]. The eccentric opening in the receiver gate was shaped to allow passage of the wire on which the sample was suspended, and yet reduce heat loss from the sample by natural convection. Normal position of the receiver in the calorimeter was such that the gage was submerged in the water. A pipe tap in the receiver allowed helium purging of both receiver and pipe connecting the receiver to the furnace.

Heat content of the sample was measured by a Parr adiabatic calorimeter. The calorimeter cover was modified to provide entrance to the receiver, inert gas tubes and gate shaft.

The temperatures in the calorimeter and in the calorimeter jacket were measured with calibrated thermometers supplied by the Parr Instrument Company. Water to the calorimeter jacket was heated by means of a 500 watt heater.

---

3. Ginnings, D. C. and R. J. Corruccini, J. of Research NBS 38, Research Paper 1797, 1947.

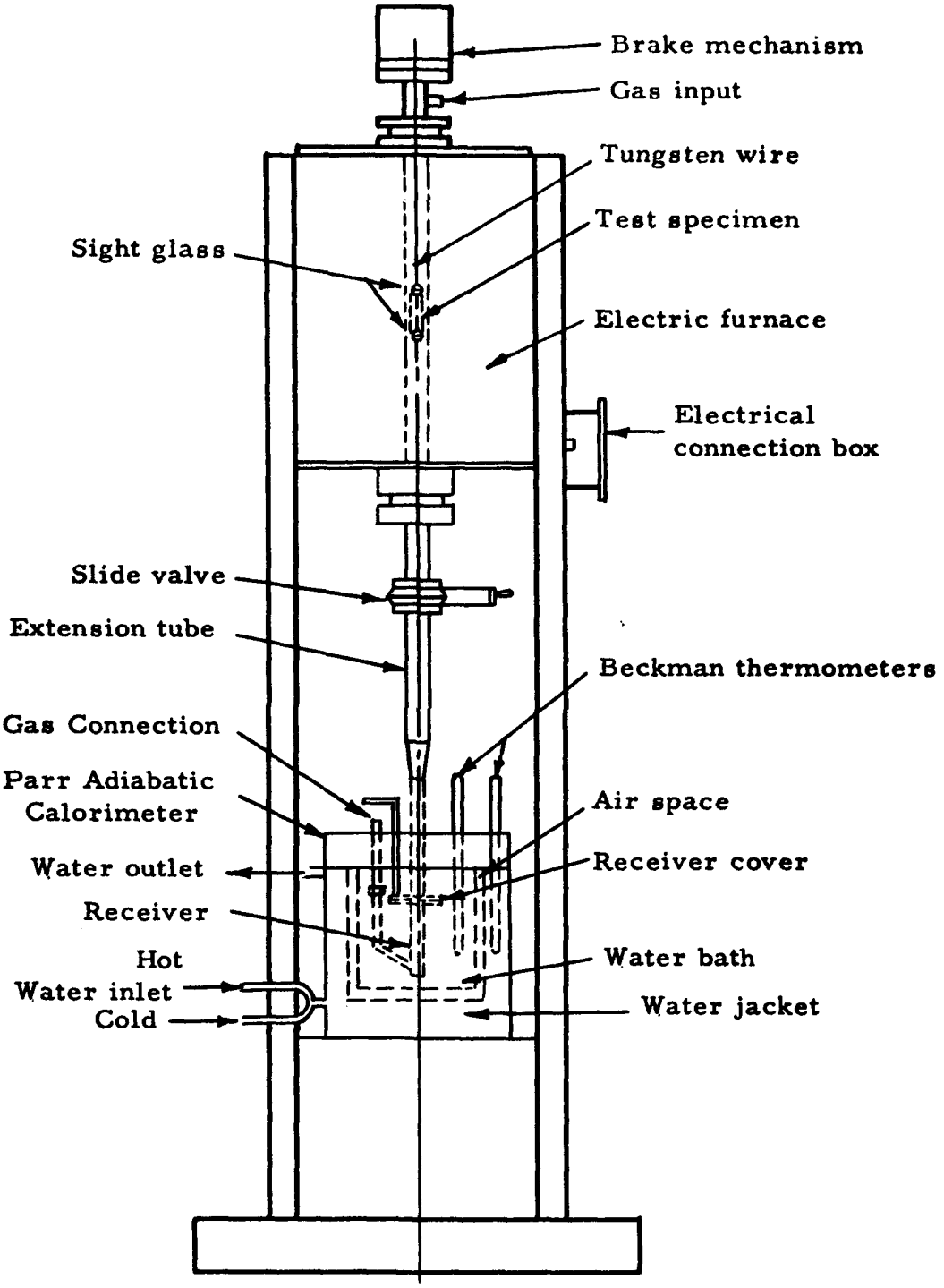

Figure 5. SCHEMATIC DIAGRAM OF APPARATUS FOR MEASURING SPECIFIC HEAT

Test Procedure

The procedure for operations of the system is outlined below. The outline is presented in chronological order:

1. The sample weight was measured using an analytical balance precise to 0.1 milligram. The sample weight was determined prior to each test.

2. The sample was then suspended in the furnace by means of a wire. The length of the wire was carefully measured before attaching the sample to assure that the sample was correctly positioned in the furnace, respective to the monitor thermocouples.

3. The sample was maintained in the furnace for 25 minutes. This time period was considered sufficient for the sample to attain thermal equilibrium. The period of time required for the sample to attain 0.95 of the difference between room temperature and furnace temperature was calculated. For a sample emissivity of 0.7 and assuming infinite sample thermal diffusivity, the period of time for 0.95 temperature rise was three minutes.

4. The weight of water contained in the bucket was measured using a pan balance precise to 0.1 gram. The bucket was then placed in the calorimeter jacket, the calorimeter cover set in position, and the calorimeter elevated to the connecting tube. The calorimeter was then brought to thermal equilibrium by equalizing the temperature level in the jacket and bucket. The receiver and connecting tube were then purged with helium.

5. The system was then in readiness for the sample drop. During the preparatory stages of this operation, the furnace thermocouple signals were recorded on a Leeds and Northrup Speedomax, which provided visual observation of in-furnace temperature behavior. Injection of the sample into the furnace caused the furnace temperature to decrease; this behavior and the subsequent rise in temperature to a non-varying level was also noted. At this point in the operation the furnace thermocouple signals were circuited to a Leeds and Northrup portable precision potentiometer; emf output to each thermocouple was determined to approximately $1^{o}F$.

6. The helium purging of receiver and connecting tube was stopped immediately before the sample drop. The gate valve at the furnace bottom was opened, the sample dropped, and the receiver gate closed. The operation from this point consisted simply in regulating the hot water input to the calorimeter jacket to maintain equal temperature level with the rising temperature level of the water in the bucket. The calorimeter attained thermal equilibrium after a period of 15 to 20 minutes, then the final temperatures were recorded.

The procedure listed above was used for all samples through the complete temperature range of operation.

Specific heat at constant pressure is defined by the equation:

$$C_p = \left| \frac{\partial(\Delta H)}{\partial T} \right|_P \qquad (2)$$

where

ΔH = enthalpy change relative to a specified datum

T = temperature

P subscript indicates the partial derivative at constant pressure.

The experimental method described here yields measurements of enthalpy change and corresponding temperature level. The relation between specific heat and the measured quantities is given by integration of Equation (2) with respect to temperature.

$$\Delta H = \int C_p \, dT = \int \left| \frac{\partial(\Delta H)}{\partial T} \right|_P dT \qquad (3)$$

The enthalpy change may be expressed in terms of a temperature function:

$$\Delta H = \phi(T)$$

Simple differentiation of $\phi(T)$ then gives C_p. The expression $\phi(T)$ used here was a quadratic of the form:

$$\Delta H = a + bT + cT^2$$

So:

$$C_p = b + 2cT$$

The enthalpy equation $\phi(T)$ was obtained from the experimental data by a least squares method. The specific heat function was determined as indicated above.

Experimental Accuracy

The selection of the function $\phi(T)$ is not based on theoretical considerations. From previous experience with treatment of enthalpy data, it has been noted that higher order equations reduce the deviation in a least squares analysis, but at the same time, the derived specific heat equations may show anomalous temperature behavior.

A suggested test of the best fit equation was given by Dr. Leo F. Epstein of General Electric Company*.

$$\left| \frac{\sum^{n} (\Delta H - \Delta H_c)^2}{n - m} \right|^{1/2} \tag{4}$$

rather than:

$$\left| \frac{\sum^{n} (\Delta H - \Delta H_c)^2}{n - 1} \right|^{1/2} \tag{5}$$

where

n = number of experimental points

ΔH = measured enthalpy at T

ΔH_c = calculated enthalpy at T

m = number of constants in enthalpy equation.

The latter equation is the deviation.

The data for synthetic sapphire was analyzed according to the relation suggested by Epstein. The two equations used in this analysis were:

$$\Delta H = -29.40 + 246.3 \times 10^{-3} T + 17.00 \times 10^{-6} T^2 \tag{6}$$

$$\Delta H = 127.5 + 291.3 \times 10^{-3} T + 9.541 \times 10^{-6} T^2 - 65.28 \log T \tag{7}$$

---

* Personal communication

The form of Eq. 7 was suggested by the most recent paper of Ginnings, et al[4]. In Eq. 6 m = 3, Eq. 7 gives m = 4. Using these values in Eq. 4, the resulting residues are:

For Eq. 6,
$$\left[\frac{\sum^{n}(\Delta H - \Delta H_c)^2}{n-m}\right]^{1/2} = 1.15 \qquad (8)$$

For Eq. 7,
$$\left[\frac{\sum^{n}(\Delta H - \Delta H_c)^2}{n-m}\right]^{1/2} = 1.91 \qquad (9)$$

As a result of this test, it is evident that there is no improvement in the results by using the added logarithmic term. For this reason Eq. 6 has been reported here.

Enthalpy and derived specific heat measurements as obtained by Eq. 6 and an equation by Ginnings, et al (loc. cit.) are compared. The NBS equation is:

$$\Delta H = 1.447978T - 1.6777 \times 10^{-5}T^2 - 460.915 \log_{10} (T + 273.16)/273.16$$

where ΔH is enthalpy change relative to 0°C, in abs. joules/gm-mol., T is temperature, °C.

A comparison between specific heat values as calculated from Eqs. 6 and 7, and the derivative of the NBS enthalpy equation is given in Table V. The NBS specific heat equation was:

$$C_p = 148.570 - 342 \times 10^{-3}T - 20{,}409.6/T$$

where C_p is expressed in abs. joules/gm mol °K, T is expressed in °K.

The agreement between the data is good in the temperature range 400 to 1700°F. The NBS equation has been extrapolated beyond 1700°F although the integral enthalpy data of NBS was done only to 1700°F.

The accuracy of the results is limited only by the accuracy of in-furnace sample temperature measurement. The measurement of heat content of the sample by the calorimeter is very precise. The temperature rise of the calorimeter was always more than 3°F; the temperature level of the calorimeter could be determined to 0.01°F. The magnitude of error from the calorimeter is probably

---

4. Ginnings, D. C. and G. T. Furukawa. J. Am. Chem. Soc. 75, 522 (1953).

TABLE V

SPECIFIC HEAT DATA FOR SYNTHETIC SAPPHIRE

(Comparison between ARF and NBS)

Temperature, °F	NBS	ARF*	ARF**
500	0.254	0.263	0.244
750	0.272	0.272	0.267
1000	0.283	0.280	0.282
1250	0.290	0.289	0.292
1500	0.296	0.297	0.301
1750	0.300	0.306	0.309

* ARF refers to derivative of Eq. 6

** ARF refers to derivative of Eq. 7

no more than 1%. This conclusion is difficult to check experimentally because it was not possible to maintain furnace temperatures constant to less than 5°F. Furnace temperature variation was caused by fluctuation in voltage input to the furnace transformers, or variation in contact resistance between the globar resistance heater and the electrode elements at the top and bottom of the globar.

Measurement of in-furnace sample temperature was accomplished by two platinum, platinum - 10% - rhodium thermocouples inserted in protection tubes. The protection tubes were necessary to prevent contamination of the thermocouples, and also to allow diffusion of oxygen down the interior of the protection tube. The validity of this measurement method was checked in the following manner. A graphite sample was axially bored to accommodate an insulated platinum, platinum - 10% - rhodium thermocouple. The sample was placed in the normal in-furnace position, and the temperatures sensed by the thermocouples enclosed in the protection tubes were compared with the thermocouple enclosed in the sample. The results of this test indicated that the temperature sensed by the sample thermocouples agreed with the arithmetic average of the temperatures sensed by protected thermocouples to 2°F. This test also served to check the contamination of the protected thermocouple: One of the protected thermocouples used in this test was new, the other had been used extensively for the previous tests. Agreement between the new and old thermocouples was excellent.

The accuracy of the derived specific heat data is difficult to state; an acceptable procedure has been to increase the standard deviation, and error of the integral enthalpy data by a factor of two. On this basis, the accuracy of the specific heat would range from 0.7 to 2.9%.

Test Results

The experimental results of the enthalpy vs temperature measurements are contained in Tables VI through VIII. Selected values of specific heat vs temperature are contained in Tables IX through XI and plotted in Figures 6 and 7.

TABLE VI

ENTHALPY VALUES FOR

0.5% TITANIUM ALLOY OF MOLYBDENUM*

Datum temperature: 80°F

Temperature, °F	ΔH_c, BTU/lb
531	33.0
720	46.7
914	56.9
1117	67.9
1278	84.5
1407	90.1
1595	101.0
1827	119.0
2013	137.0
2166	144.0
2385	165.0
2528	181.0
2670	184.0
2820	207.0

* Experimental data

$$\Delta H = 6.50 + 48.1 \cdot 10^{-3}T + 7.79 \cdot 10^{-6}T^2$$

TABLE VII

ENTHALPY VALUES FOR

ATJ GRAPHITE*

Datum temperature: 80°F

Temperature, °F	ΔH_o, BTU/lb
660	139
321	218
1015	285
1190	361
1443	468
1611	530
1795	602
2005	712
2207	805
2386	879
2527	950
2691	1029
2876	1131

* Experimental data

$$\Delta H = -94 + 349 \cdot 10^{-3}T + 25.9 \cdot 10^{-6}T^2$$

TABLE VIII

ENTHALPY VALUES FOR

SILICONIZED ATJ GRAPHITE*

Datum temperature: 80°F

Temperature, °F	ΔH_c, BTU/lb
660	103
821	151
1015	235
1190	314
1443	414
1611	472
1795	573
2005	660
2207	749
2386	841
2527	895
2691	991
2876	1067

* Experimental data

$$\Delta H = -144 + 349 \cdot 10^{-3}T + 25.9 \cdot 10^{-6}T^2$$

TABLE IX

SELECTED VALUES OF SPECIFIC HEAT FOR

0.5 PERCENT TITANIUM ALLOY OF MOLYBDENUM

Temperature, ^{o}F	C_p, BTU lb^{-1} F^{-1}
800	0.060
1200	0.067
1600	0.073
2000	0.079
2400	0.086
2800	0.092

$$C_p = 0.0481 + 0.0156 \cdot 10^{-3}T$$

TABLE X

SELECTED VALUES OF SPECIFIC HEAT FOR

ATJ GRAPHITE

Temperature, ^{o}F	Specific Heat BTU lb^{-1} F^{-1}
800	0.390
1200	0.411
1600	0.432
2000	0.453
2400	0.473
2800	0.494

$$C_p = 0.349 + 0.0518 \cdot 10^{-3}T$$

TABLE XI

SELECTED VALUES OF SPECIFIC HEAT FOR

SILICONIZED ATJ GRAPHITE

Temperature, ^{o}F	Specific heat, BTU lb^{-1} F^{-1}
800	0.390
1200	0.411
1600	0.432
2000	0.453
2400	0.473
2800	0.494

$$C_p = 0.349 + 0.0518 \cdot 10^{-3}T$$

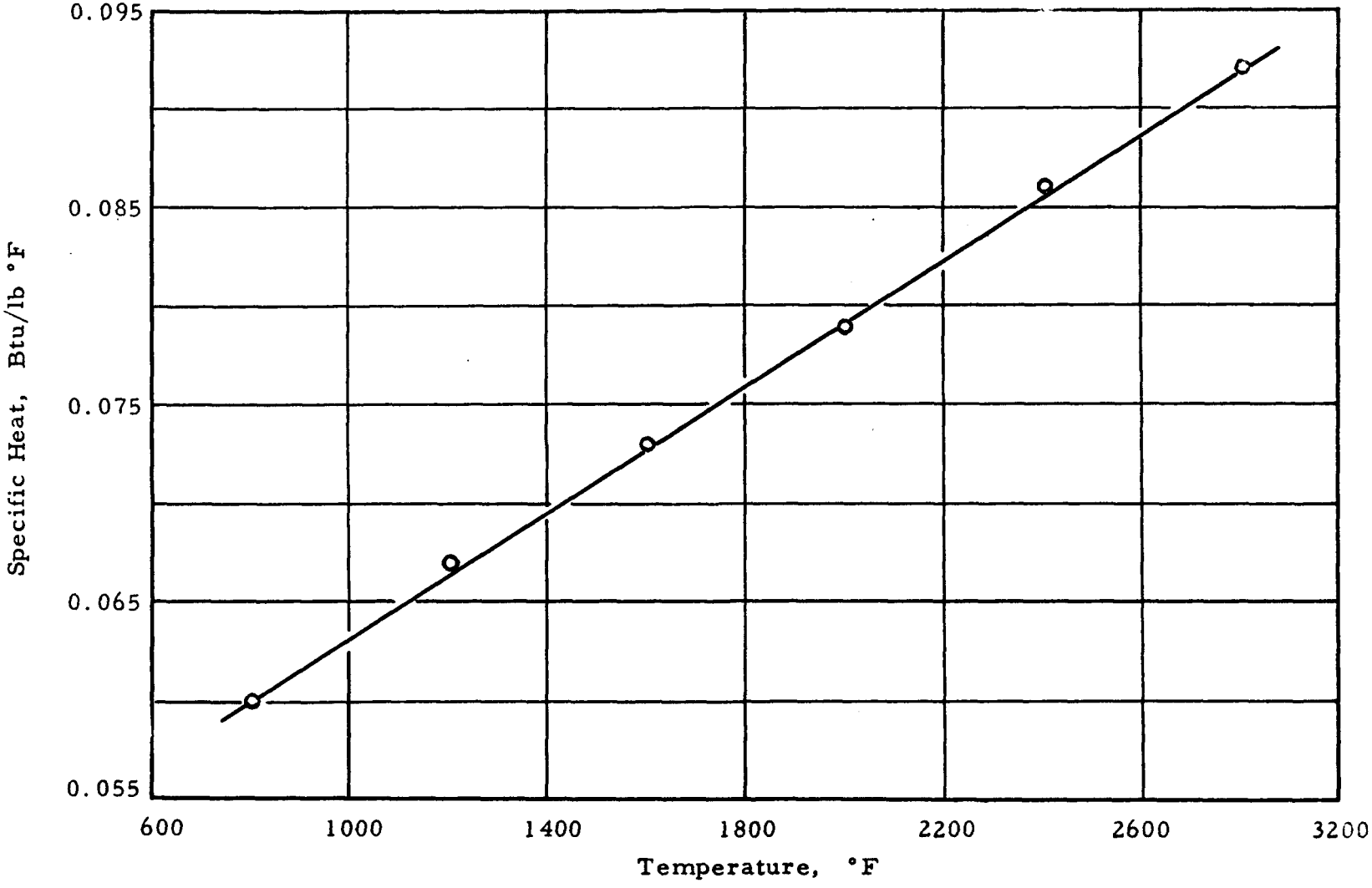

Figure 6. SPECIFIC HEAT OF 0.5% TITANIUM ALLOY OF MOLYBDENUM

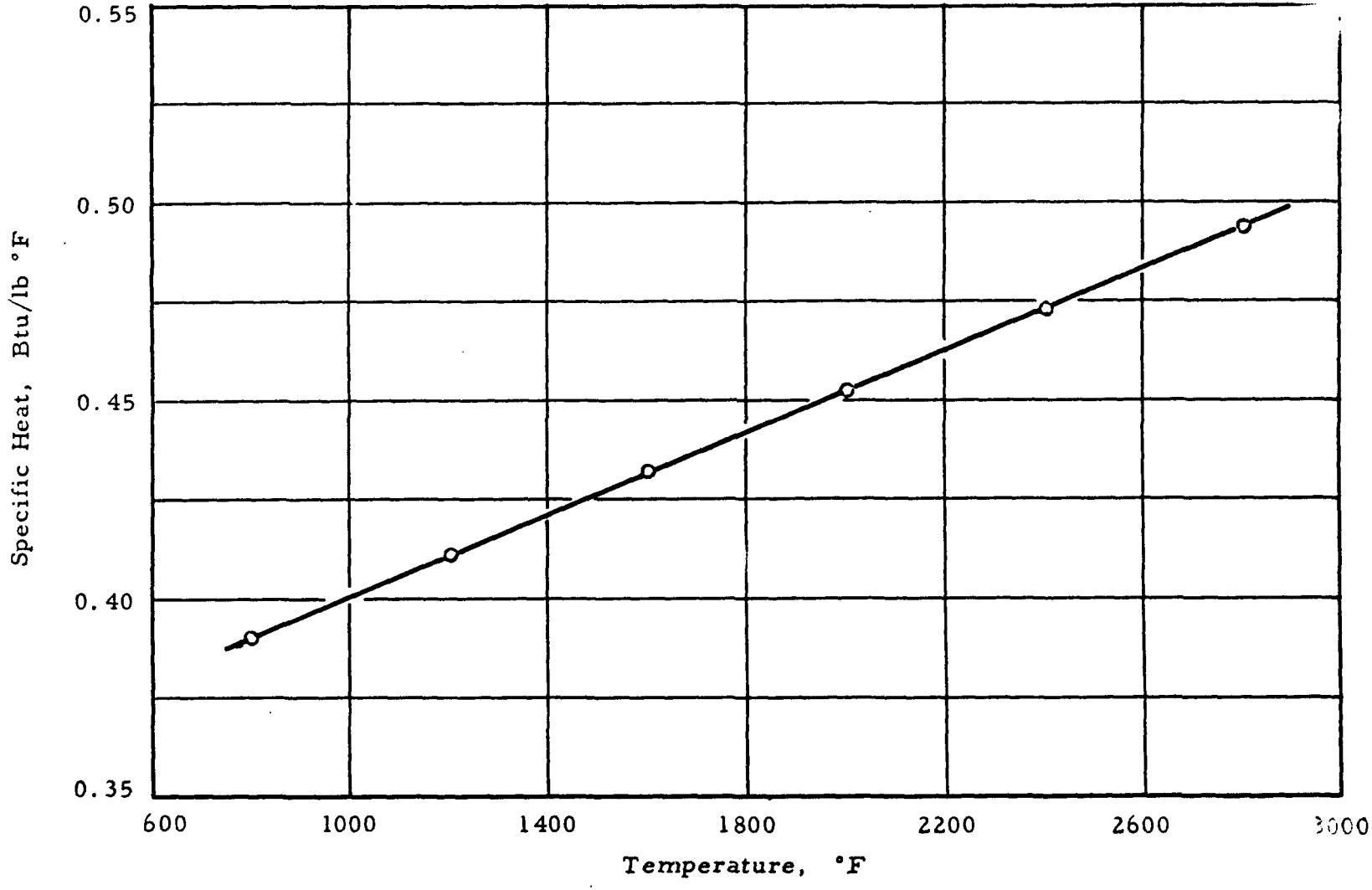

Figure 7. SPECIFIC HEAT OF SILICONIZED ATJ GRAPHITE

IV. LINEAR THERMAL EXPANSION

Description of Equipment

The linear thermal expansion was determined by measuring the distance between two recrystallized alumina pins mounted in a rod of material to be evaluated.

A schematic diagram of the apparatus is shown in Figure 8. The furnace is heated by three banks of globar elements at the front, middle, and rear of the furnace. Each bank of globar elements may be heated independently so as to insure a uniform temperature along the middle of the furnace. Preliminary tests indicated that the variation of temperature of the specimens along their length was within 5°F. The furnace temperature was measured by platinum, platinum - 10% - rhodium thermocouples located one inch from either end of the sample and the sample temperature was measured by a thermocouple located in one end of the specimen.

The specimen is mounted in a ceramic tube in the center of the furnace, with the ceramic pins pointing upward. In this position the line-up is such that the pins may be seen from outside the furnace and the distance between them measured directly with the telemicroscope. During the lower temperature portions of each run, the pins are silhouetted against a lighted white background behind the furnace. Once the interior of the furnace begins to get cherry red, the lights are turned off and the red pins are easily seen against the now dark background. A slow stream of helium is maintained into the ceramic tube supporting the sample to protect the sample from oxidation.

The telemicroscopes are mounted on an Invar bar which has a very low coefficient of thermal expansion and the displacements of the pins are read by means of a micrometer to an accuracy of 0.0001 inch. The complete assembly is shock mounted to minimize vibrations.

Test Procedure

The procedure for operation of the apparatus is outlined below. The outline is presented in chronological order.

1. Two holes are drilled 10 inches apart through a rod of the specimen 1/2 inch in diameter and 11 inches long.

2. A thermocouple is located in a 0.020 inch hole at one end of the specimen.

Figure 8. APPARATUS FOR MEASURING LINEAR THERMAL EXPANSION

3. Two ceramic pins are mounted in the holes in the specimen and project out about 1/8 inch from them.

4. The specimen is mounted in the ceramic tube in the furnace with the pins pointing up.

5. The end cap on the furnace is then closed, and helium gas is fed to the ceramic tube supporting the sample.

6. Heat is supplied to the furnace and temperature and pin displacement measurements are made at regular time intervals. The rate of heating may be varied from 0 to 100°F per hour and still give consistent test results.

Experimental Accuracy

The measurement of thermal expansion is an absolute measurement and hence all errors are inherent in the apparatus and observer, such as incorrect temperature measurements or variations in the optical system. These sources of error are considered to be relatively small (less than 3%) and of a random nature.

Test Results

The thermal expansion was measured from 70°F to 3000°F. The linear thermal expansion and mean coefficients of expansion from 70°F to various temperatures are given in Tables XII, XIII and XIV and are shown graphically in Figures 9 through 13.

TABLE XII

LINEAR THERMAL EXPANSION OF 0.5% TITANIUM ALLOY OF MOLYBDENUM

Temperature	$\frac{\Delta L}{L}$, % *	Mean Coeff. x 10^6 in/in °F
70	0.0	
70 - 100		2.840
70 - 200	0.036	2.865
70 - 300	0.068	2.890
70 - 400	0.095	2.920
70 - 500	0.127	2.940
70 - 600	0.158	2.970
70 - 700	0.189	3.000
70 - 800	0.219	3.025
70 - 900	0.253	3.050
70 - 1000	0.286	3.080
70 - 1100	0.318	3.115
70 - 1200	0.353	3.135
70 - 1300	0.388	3.165
70 - 1400	0.427	3.200
70 - 1500	0.463	3.230
70 - 1600	0.500	3.260
70 - 1700	0.529	3.290
70 - 1800	0.577	3.325
70 - 1900	0.618	3.355
70 - 2000	0.658	3.390
70 - 2100	0.678	3.425
70 - 2200	0.737	3.460
70 - 2300	0.783	3.495
70 - 2400	0.825	3.535
70 - 2500	0.869	3.570
70 - 2600	0.913	3.615
70 - 2700	0.958	3.655
70 - 2800	1.005	3.695
70 - 2900	1.056	3.720
70 - 3000	1.110	3.780

*Experimental Data

TABLE XIII

LINEAR THERMAL EXPANSION OF SILICONIZED ATJ GRAPHITE

(Sample No. 1)

Temperature	$\frac{\Delta L}{L}$, % *	Mean Coeff. x 10^6 in/in °F **
70	0.0	
70 - 100		1.775
70 - 200	0.027	1.790
70 - 300	0.045	1.800
70 - 400	0.054	1.815
70 - 500	0.084	1.825
70 - 600	0.098	1.845
70 - 700	0.117	1.865
70 - 800	0.134	1.880
70 - 900	0.153	1.900
70 - 1000	0.175	1.925
70 - 1100	0.201	1.945
70 - 1200	0.223	1.970
70 - 1300	0.247	1.995
70 - 1400	0.269	2.020
70 - 1500	0.292	2.045
70 - 1600	0.318	2.075
70 - 1700	0.343	2.100
70 - 1800	0.368	2.125
70 - 1900	0.395	2.150
70 - 2000	0.420	2.175
70 - 2100	0.448	2.200
70 - 2200	0.475	2.225
70 - 2300	0.502	2.250
70 - 2400	0.530	2.279
70 - 2500	0.564	2.298
70 - 2600	0.588	2.320
70 - 2700	0.618	2.345
70 - 2800	0.648	2.370
70 - 2900	0.678	2.390
70 - 3000	0.710	2.415

* Experimental Data

** Data shows some scatter from 70°F to 1000°F

TABLE XIV

LINEAR THERMAL EXPANSION OF SILICONIZED ATJ GRAPHITE

(Sample No. 2)

Temperature	$\frac{\Delta L}{L}$, % *	Mean Coeff. x 10^6 in/in °F **
70	0.0	
70 - 100		0.01
70 - 200	0.007	0.15
70 - 300	0.010	0.39
70 - 400	0.020	0.63
70 - 500	0.036	0.83
70 - 600	0.054	1.02
70 - 700	0.079	1.21
70 - 800	0.103	1.38
70 - 900	0.129	1.52
70 - 1000	0.153	1.64
70 - 1100	0.179	1.73
70 - 1200	0.207	1.81
70 - 1300	0.232	1.88
70 - 1400	0.258	1.94
70 - 1500	0.285	1.99
70 - 1600	0.312	2.04
70 - 1700	0.340	2.07
70 - 1800	0.367	2.11
70 - 1900	0.395	2.15
70 - 2000	0.422	2.18
70 - 2100	0.450	2.21
70 - 2200	0.479	2.24
70 - 2300	0.507	2.26
70 - 2400	0.535	2.28
70 - 2500	0.562	2.30
70 - 2600	0.592	2.32
70 - 2700	0.621	2.35
70 - 2800	0.649	2.37

* Experimental Data
** Data shows some scatter from 70°F to 1000°F

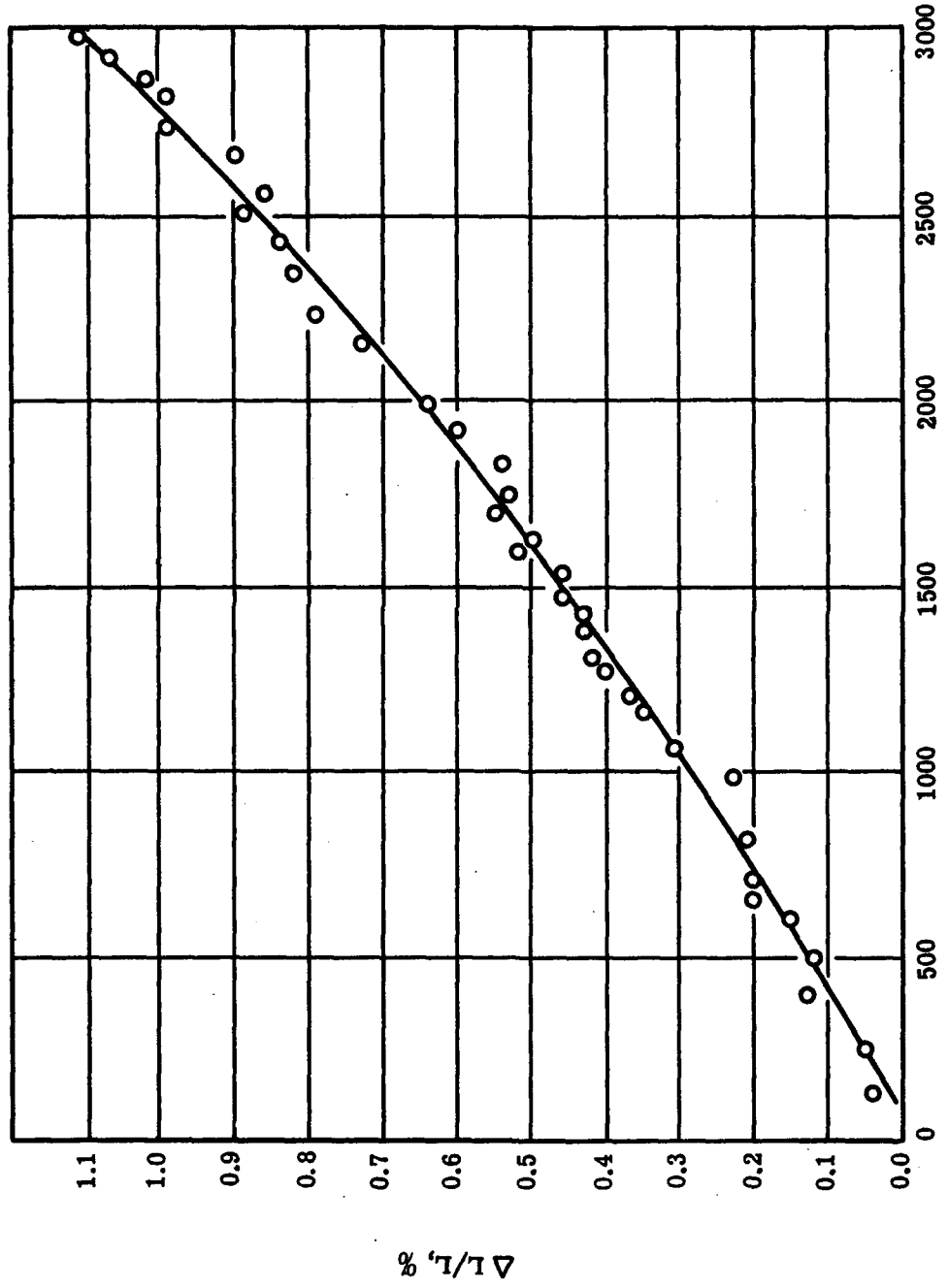

Figure 9. LINEAR THERMAL EXPANSION OF 0.5% TITANIUM ALLOY OF MOLYBDENUM

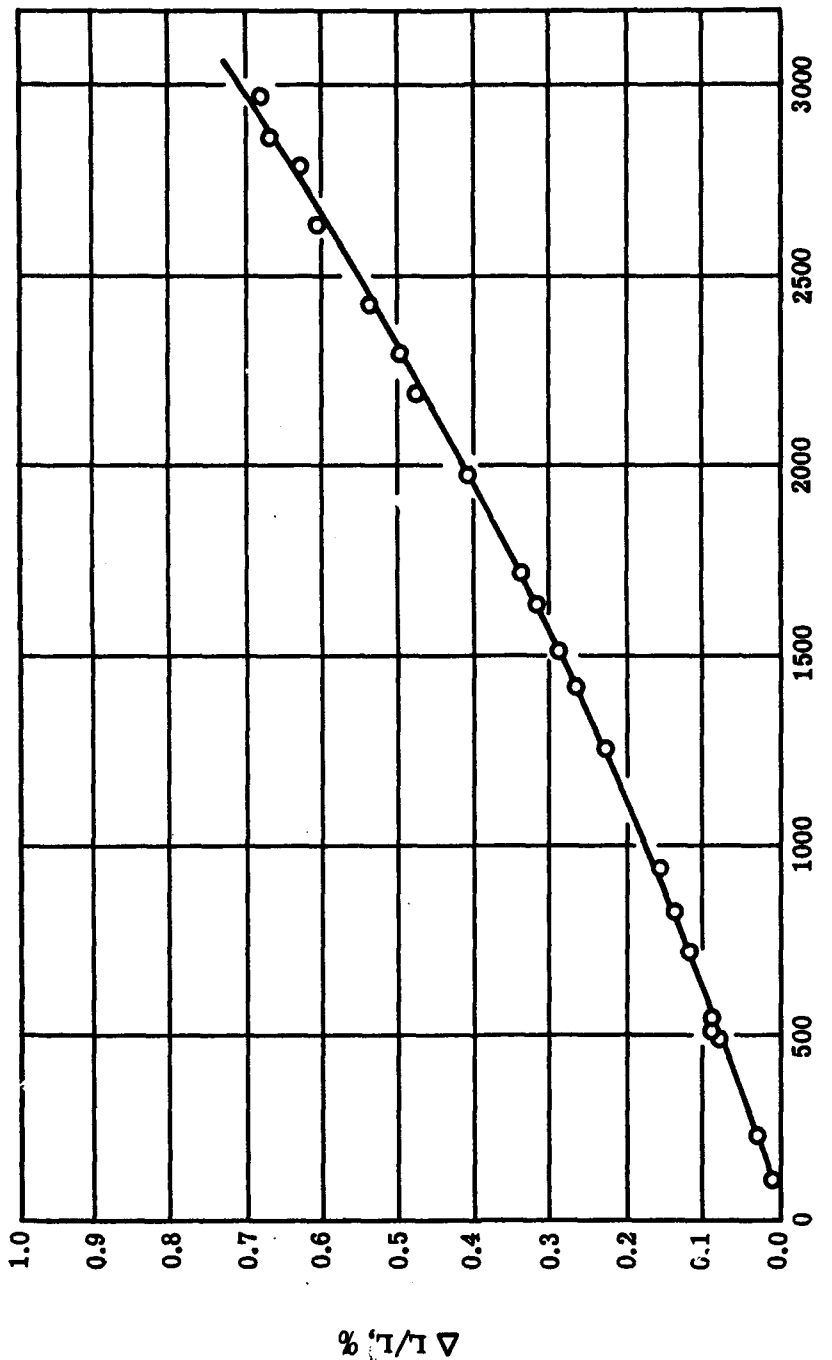

Figure 10. LINEAR THERMAL EXPANSION OF SILICONIZED ATJ GRAPHITE
Sample 1

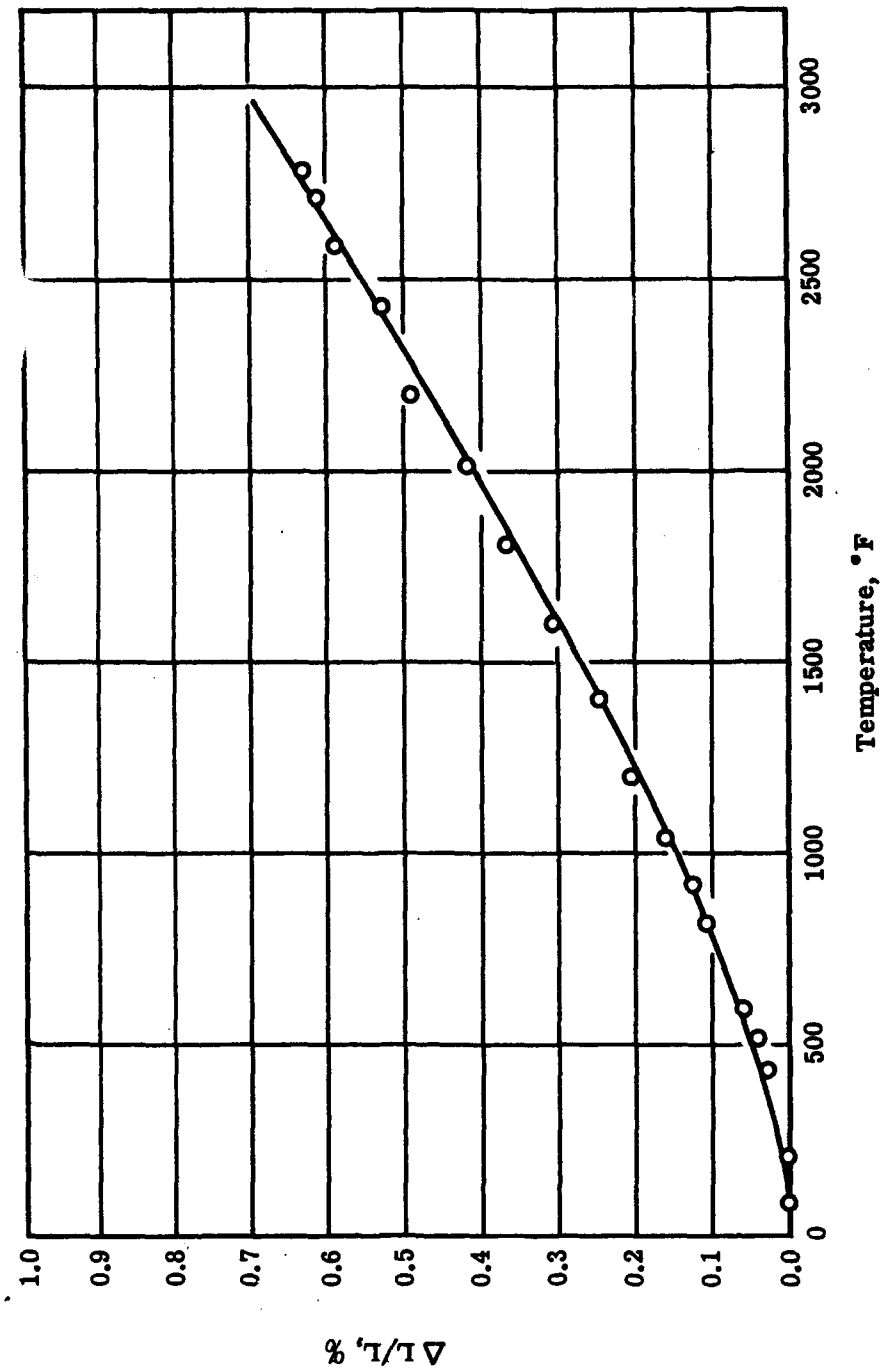

Figure 11. LINEAR THERMAL EXPANSION OF SILICONIZED ATJ GRAPHITE
Sample 2

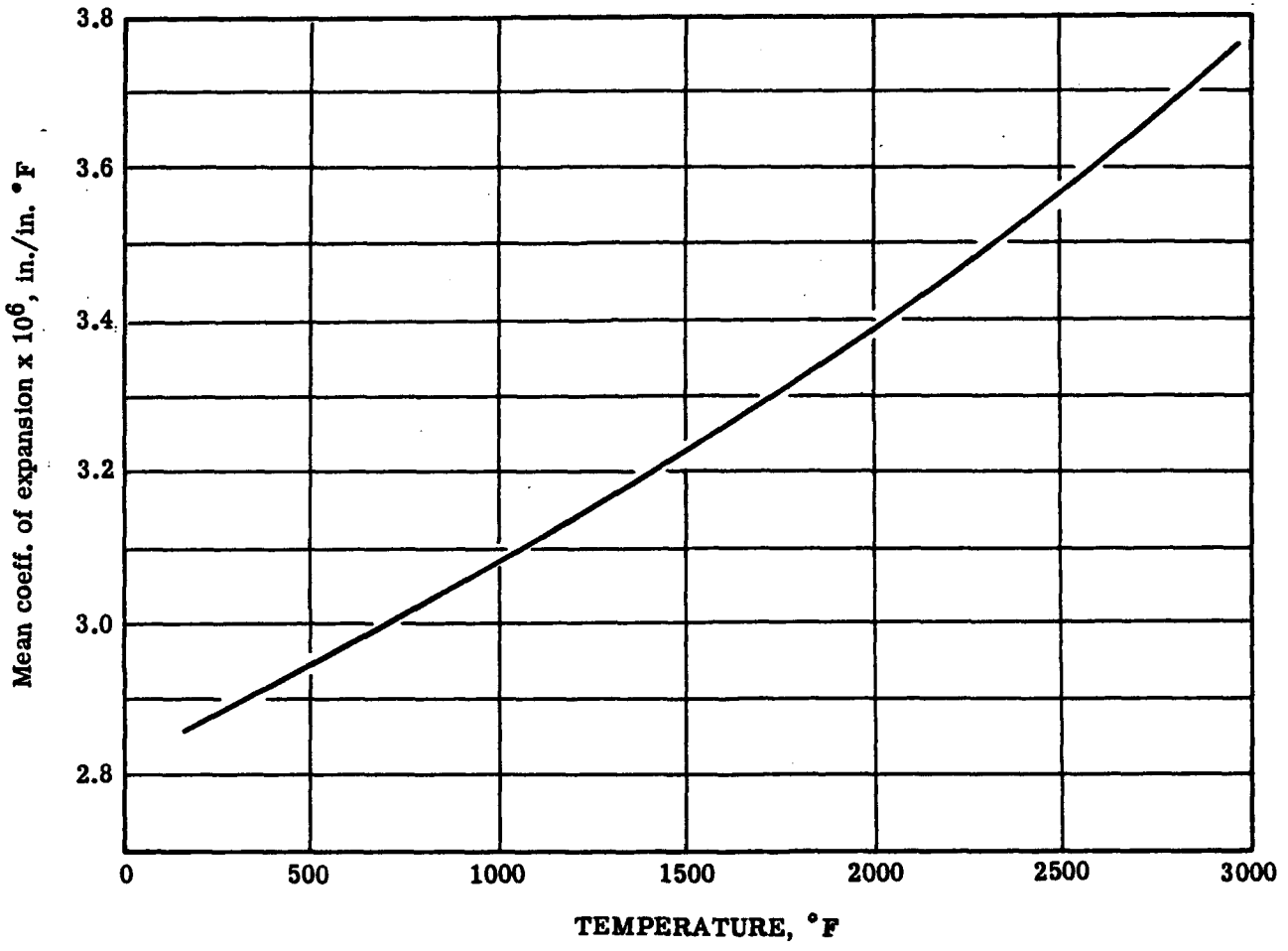

Figure 12. MEAN COEFFICIENT OF LINEAR THERMAL EXPANSION (ABOVE 70°F) OF 0.5% TITANIUM ALLOY OF MOLYBDENUM

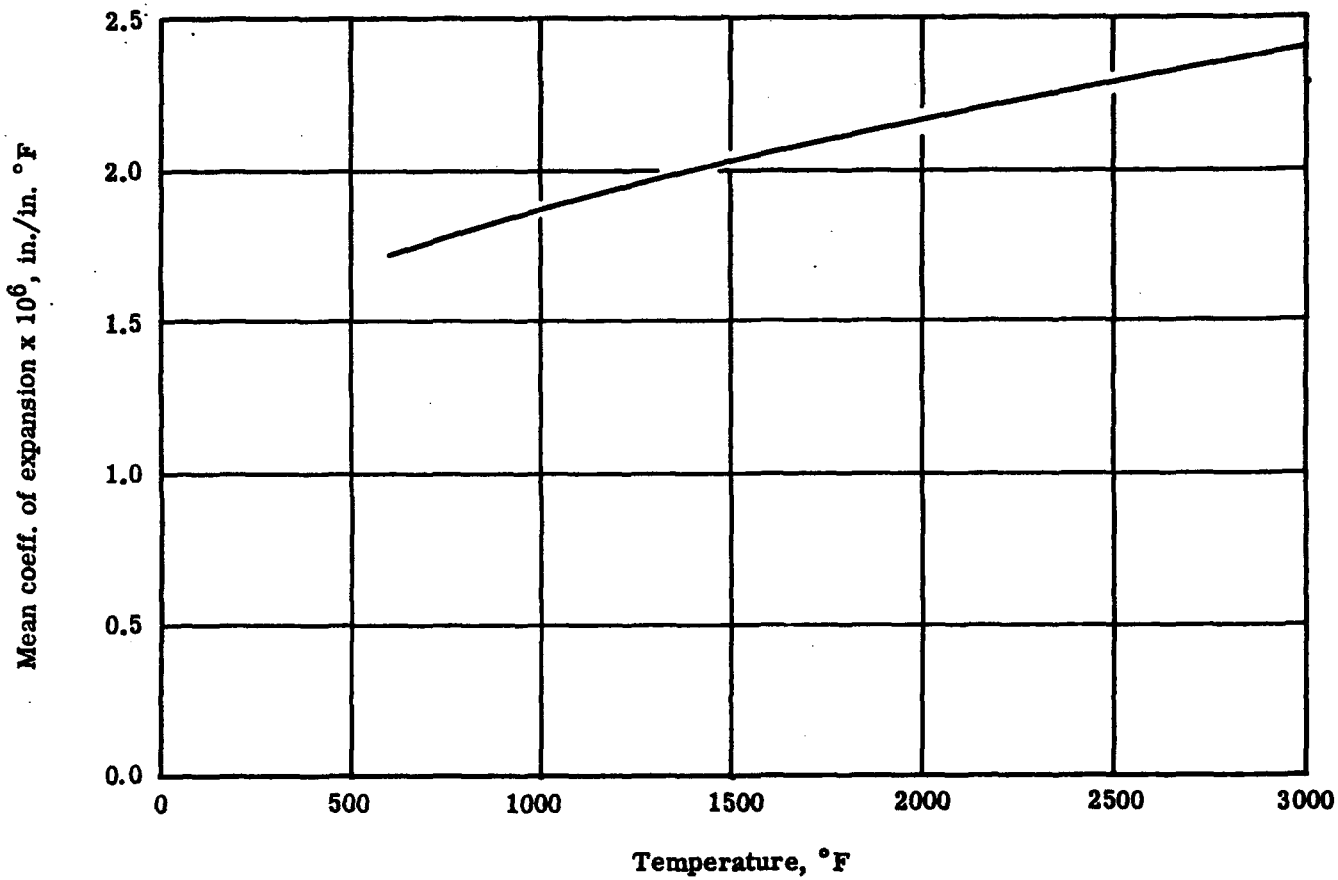

Figure 13. MEAN COEFFICIENT OF LINEAR THERMAL EXPANSION (ABOVE 70°F) OF SILICONIZED ATJ GRAPHITE

V. THERMAL EMISSIVITY

By

Henry R. Blau, Jr., Eleanor Chaffee,
John R. Jasperse and William S. Martin
Arthur D. Little, Inc.
Cambridge, Massachusetts

A. DESCRIPTION OF EQUIPMENT

1. Theory

The total power W radiated per unit surface area by a material at temperature T is

$$W = \bar{\epsilon}(T)\sigma T^4 = \bar{\epsilon}(T)W_b \qquad (10)$$

where $\bar{\epsilon}(T)$ is the total hemispherical emissivity, σ the Stephan-Boltzmann constant, and $W_b = \sigma T^4$ is the total power radiated by a perfect radiator or black body at temperature T.

From Equation 10 it is apparent that quantitative expression of the power radiated by leading edge materials hinges on accurate knowledge of total hemispherical emittance in the temperature range of interest.

Practical difficulties are encountered if one attempts to measure total hemispherical emittance directly. These difficulties are avoided if a related parameter the total angular emittance $\bar{\epsilon}_\theta(T)$ defined according to Equation 11 is determined.

$$\bar{\epsilon}_\theta(T) = \frac{W_\theta}{W_{b\theta}} \qquad (11)$$

In Equation 11 the subscript θ refers to radiation emitted at a single angle θ from the normal to the surface. The surface of most materials of interest in leading edge applications is "optically" rough. It has been observed that such materials are cosine emitters, that is, $\bar{\epsilon}_\theta$ is constant for all angles of emission. Significant departures from cosine emission have been observed for optically polished metals and dielectrics. For this reason it was decided to carry out measurement of $\bar{\epsilon}_\theta(T)$ at the angles of emission of θ, 0^o, 30^o, 45^o, and 60^o, from the outward drawn normal to the material surface. If, as expected, the values of $\bar{\epsilon}_\theta(T)$ are found to be equal at all four angles, it may be assumed that the material is a cosine emitter. If cosine emission is not observed, the total hemispherical emittance must be determined by numerical integration from angular values.

The thermal emittance $\bar{\epsilon}_\theta(T)$ can be determined directly by comparing W_θ, the radiation emitted by the sample at angle θ, with $W_{b\theta}$, the radiation emitted by a black body at the same temperature and at the same angle. Because of its simplicity this approach is ordinarily utilized at moderate temperatures.

At high temperatures in excess of about 1300F direct measurement of $\bar{\epsilon}_\theta(T)$ is no longer possible because of the unavailability of suitable black-body reference standards. At these high temperatures $\bar{\epsilon}_\theta(T)$ is calculated from black-body relation ($W_{b\theta} = \frac{\sigma T^4}{\pi} \cos\theta$) and from experimental values of T and W_θ. The high temperature method has been used throughout this program. The accuracy of the method hinges on the requirement for absolute measurement of sample temperature and absolute measurement of W_θ, the total power radiated by the sample per unit surface area, per unit solid angle at angle θ.

Above about 1300F accurate surface temperatures can be determined with an optical pyrometer if the sample emittance at 0.65 microns is known or if black-body conditions can be provided. Since accurate values of spectral emittance at 0.65 microns, the wavelength of operation of the pyrometer, are available for only a few materials, temperatures were measured by sighting on a small black-body cavity drilled in the sample surface.

Absolute measurement of W_θ was achieved by careful calibration of the radiation sensor against a precision black-body reference standard. Since the emissive properties of the black-body standard are known, it was possible to directly relate detector response to incident power. Using this relation the signal produced by radiation from a sample material at a particular temperature T could be expressed as power per unit area per unit solid angle and total angular emittance $\bar{\epsilon}_\theta(T)$ calculated from Equation (11). A detailed discussion of the accuracy of measurement of T, W_θ, and $\bar{\epsilon}_\theta(T)$ will be given in Section C.

2. Apparatus

The essential features of the apparatus used for total emittance measurements are:

a. A source unit in which the sample is heated to the desired high temperature in a controlled atmosphere,

b. external optics used to collect radiation emitted by the hot sample,

c. a radiation sensing system used to measure the intensity of emitted radiation,

d. a black-body standard for absolute calibration, and

e. a micro-optical pyrometer for sample temperature measurement.

Figure 14 is a schematic diagram of the apparatus showing these components. Radiation emitted by the hot sample is focused on the 10 cycle chopper B by plane mirror M_1 and spherical mirror M_2. The chopped radiation in turn is

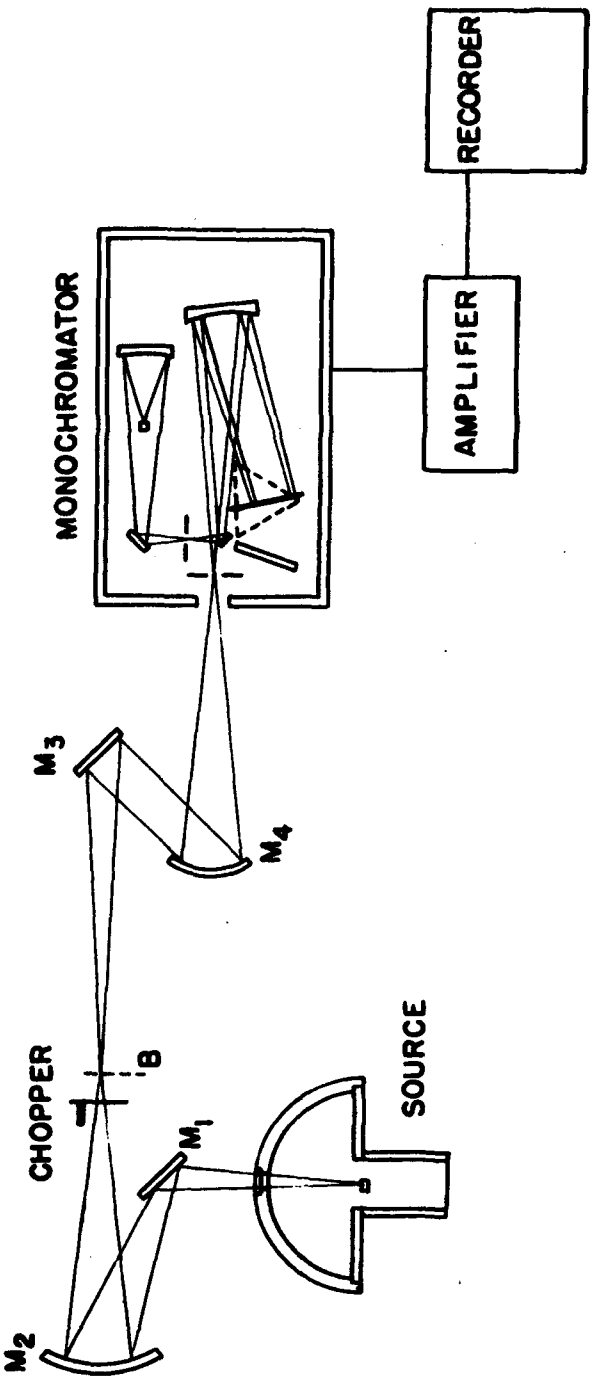

Figure 14. A SCHEMATIC DIAGRAM OF THE EMISSIVITY APPARATUS

focused on the entrance slit of a Perkin-Elmer monochromator by mirror combination M_3 and M_4. Radiation transmitted by the entrance slit of the monochromator is brought to a focus on the thermocouple detector by the monochromator optics. (Since total rather than spectral radiation was to be measured, the prism ordinarily used to disperse the incoming radiation was removed and replaced by a plane mirror). Finally the alternating signal generated by the thermocouple is amplified, synchronously rectified, and displayed on a strip chart recorder in the usual manner.

(1) Source Unit

The source unit consists of an induction furnace* and an evacuable chamber and gas handling system that permits heating the sample in any desired atmosphere. Details of the source unit are shown in Figure 15.

The induction furnace consists of a primary RF coil surrounding a pyrex cylinder that in turn surrounds a water-cooled concentrator. The concentrator is a thin cylindrical shell open on one end. The other end is closed except for a circular opening at the center that is slightly larger in diameter than the sample. A narrow slot in the concentrator shell runs from the edge of the circular opening across the top plate and down the side wall.

The sample**, a disk 3/8" in diameter and 3/16" in thickness is mounted coaxially with the concentrator and supported by a zirconia rod. The upper surface of the sample is maintained slightly below the outer surface of the concentrator. The pyrex cylinder surrounding the concentrator is sealed below to a base plate and above to a brass hemicylinder with neoprene "O" rings. NaCl windows are located in the curved surface of the hemicylinder directly above the sample (0°), and at angles of 30°, 45°, and 60° from the normal to the sample.

The hemicylinder is so arranged that it can be rotated about an axis passing through the center of the sample in the plane of the sample surface. Since the optics used to focus emitted radiation on the sample (Figure 14) are fixed in position, this arrangement permits accurate measurement of the dependence of emittance on angle at the four angles 0°, 30°, 45°, and 60° from the normal.

(2) Radiation Sensing System

A modified Perkin-Elmer Model 12 spectrograph was used to measure the radiant intensity emitted by sample materials. As mentioned previously, the prism was removed from the instrument and replaced by a plane, front surfaced mirror. The plane mirror was oriented so that the entrance slit was imaged on the exit slit and total radiation reached the detector. In essence the modified spectrograph served as a variable aperture (entrance slit) followed by an optical system that focused radiation transmitted by the entrance slit on a high quality, evacuated Perkin-Elmer thermocouple detector.

---

*The induction furnace was a modified Sylvania 7 kva Induction Light Source RS-1.
**Appendix I, Figure

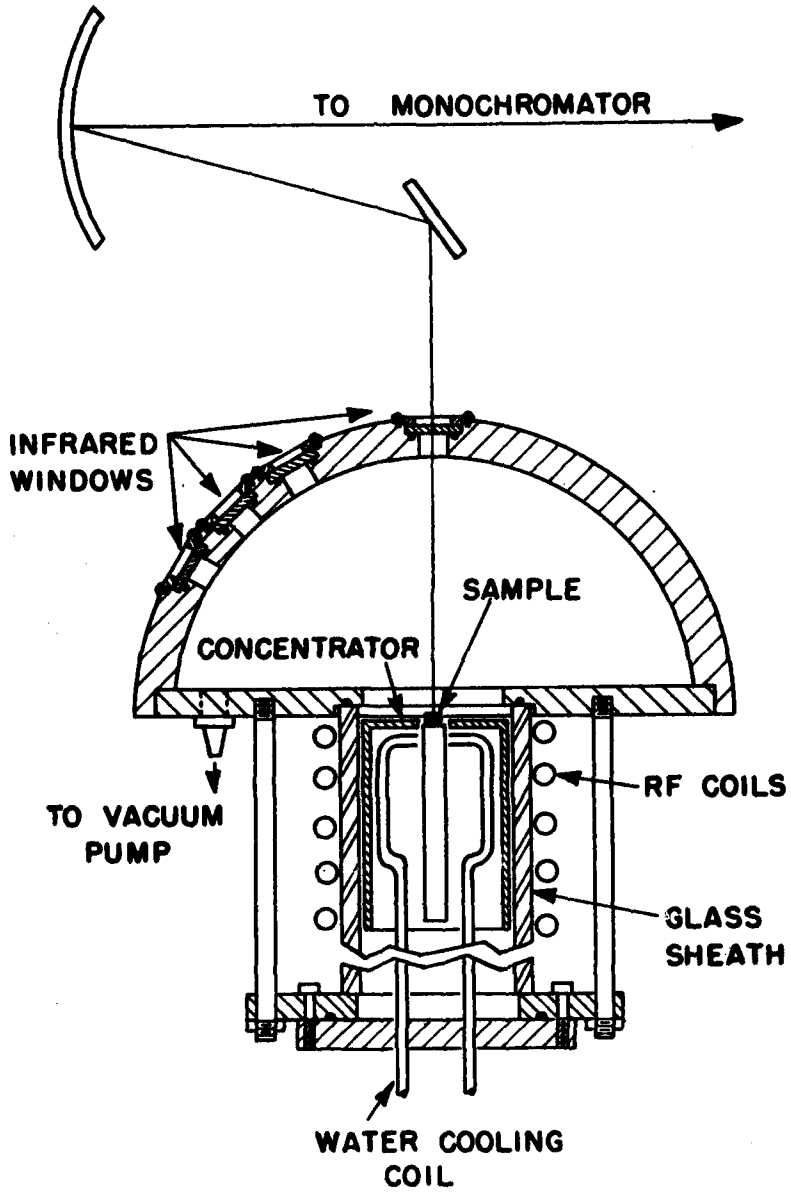

Figure 15. A SCHEMATIC DIAGRAM SHOWING DETAILS OF THE SOURCE UNIT

The vertical height of the entrance slit was reduced by field stops to a height of approximately 1 mm. The area of the slit-aperture was varied in a known manner by means of the slit micrometer in such a way as to maintain a reasonable flux level at the detector over the temperature range of interest. The surface area of the sample viewed by the detector was approximately 1 mm x 0.5 mm at normal emission.

The amplifier used with the spectrometer is so designed that known, low-level, test signals can be introduced across the detector. The test signals were used to determine the linearity of the amplifier-recorder system over the gain range of interest. In addition the test signals were used several times in the course of a run to check the response of the electronic network. Since the electronic network is the chief source of instability in the measuring system, this procedure avoided systematic errors due to changes in tube characteristics, line voltages, and the like. When electronic instabilities were taken into account, it was found that an accurate absolute calibration could be maintained for several weeks or more providing that the optical alignment was not modified.

(3) Temperature Measuring Instruments

Above 1300F the sample temperature was measured with a disappearing filament type, micro-optical pyrometer sighting through the NaCl window on a small black-body cavity drilled in the sample surface. Precautions were taken (Section C) to obtain near black-body conditions in the cavity and to take into account attenuation of sample radiation reaching the pyrometer produced by the NaCl window and other optical elements. The NaCl windows used were 6 mm thick and carefully polished. They transmit radiation in the wavelength range of 0.2 to 15 microns.

Below 1300F attempts were made to measure sample temperatures with a fine, 5 mil platinum-platinum, 10% rhodium thermocouple imbedded in the sample. The 5 mil wire was used to minimize the conductive heat leak along the thermocouple wires and the junction was imbedded as deeply as possible in the sample.

Although considerable efforts were devoted to the thermocouple measurements, in no case were really satisfactory results obtained. At elevated temperatures both thermocouple and pyrometer temperatures were recorded so that the two measuring techniques could be compared, thermocouple temperatures were found to be lower than pyrometer temperatures; the difference in the two temperatures increased as the sample temperature decreased. The temperature difference between the two measuring techniques ranged from 100F to no more than 200F.

The temperature differences are attributed to the heat leak afforded by the thermocouple wires. The observed temperature differences support this view. At high temperatures radiation losses are more important than conductive losses, and the temperature difference is small. At lower temperatures the conductive loss becomes increasingly important and the temperature differences increase. Because of this situation, it was not possible to determine accurate temperatures and, hence, emittances in the 500F-1000F range.

(4) Black-body Standards

A Barnes RS-3A high temperature black-body standard (ϵ = .99 ±1%, ΔT ±6°F) was used for calibration purposes up to 1100F and siliconized graphite at higher temperatures. During calibration the induction furnace was removed and replaced by the black-body standard. Care was taken to ensure that the black-body aperture was precisely located at the sample position. However, since the diameter of the black-body aperture was substantially larger than the diameter of the area on the surface viewed by the detector, the calibration constant was found to be relatively insensitive to the location of the black-body aperture.

B. TEST PROCEDURE

1. Absolute Flux Measurement

The voltage response V of the system to a source of total emissive power W_θ for a given angle θ is

$$V = (W_\theta - W_o) \left[k\Omega T' H\right] S \tag{12}$$

where W_o is the total emissive power of the chopper blade, k is the sensitivity of the detector (volts/watt), Ω is the solid angle viewed by the detector, T' is the effective transmissivity of the optical system, H is the optical height of the entrance slit, and S is the optical width of the same slit. The product in square brackets is a constant for the system and may be replaced by

$$C^{-1} = \left[k\Omega T' H\right] \tag{13}$$

where C is the calibration constant.

For source temperature above about 1000F, $W_\theta >> W_o$, and the W_o term may be neglected. Equation (12) then becomes

$$V = W_\theta C^{-1} S \tag{14}$$

The calibration constant C can be determined experimentally by observing the system response to a source of known intensity such as a black-body standard according to

$$C = \frac{W_{b\theta} S}{V_b} \tag{15}$$

where V_b is the voltage response produced by the black-body flux $W_{b\theta}$.

The "optical" slit width S differs from the physical slit width S_M as read on the slit micrometer. The difference results from diffraction at the slit and must be taken into account. Diffraction at the aperture deflects radiation from the collimated beam and hence reduces the flux reaching the detector. For a given slit width the degree of diffraction depends on the wavelength of the incident radiation. When the wavelength is such that $\lambda \geq S$, diffraction will be quite important. On the other hand, when $\lambda << S$, diffraction will be negligible.

At low temperatures the radiation emitted by a black-body is low in intensity and is concentrated at long wavelengths. As the black-body temperature increases, the emitted intensity increases and proportionally more radiation is emitted at short wavelengths. Consequently, a slit that is sufficiently narrow to completely attenuate radiation from a cool source will transmit a fraction of the radiation from a hot source. In other words, the effective slit width required for zero transmission is smaller the greater the source temperature. The optical slit width S (Equation 13) can be written

$$S = S_M - S_o(T) \tag{16}$$

where S_M is the effective slit closure. With this notation Equations (12) and (15) become respectively

$$V = W_\theta C^{-1}(S_M - S_o(T)) \tag{17}$$

and

$$C = \frac{W_{b\theta}(S_M - S_o(T))}{V_b} \tag{18}$$

Values of $S_o(T)$ were determined from the intercepts of plots of the instrument voltage response R vs S_M for various constant source temperatures. The black-body standard served as source at temperatures below 1100F. Higher temperature data were obtained by using a siliconized graphite sample heated in the induction furnace. This course was adopted because of the near gray-body emission characteristics of this material. Figures 16 and 17 are graphs of R vs S_M for a number of source temperatures, while Figure 18 is a graph of $S_o(T)$ vs T. The values of $S_o(T)$ were obtained from the intercepts in Figures 16 and 17.

Once having determined values of $S_o(T)$ for the temperature range of interest, the calibration constant was determined by using Equation (13) and experimental values of R_b, S_M, and $S_o(T)$. Figure 19 is a graph of calibration constant C vs T so obtained. The calibration constant obtained from Figure 19 was used at temperatures from 1100-3000F with the $S_o(T)$ values determined with siliconized graphite in the same temperature range. With the calibration constant and slit function, total emittances were determined according to Equations (11) and (17).

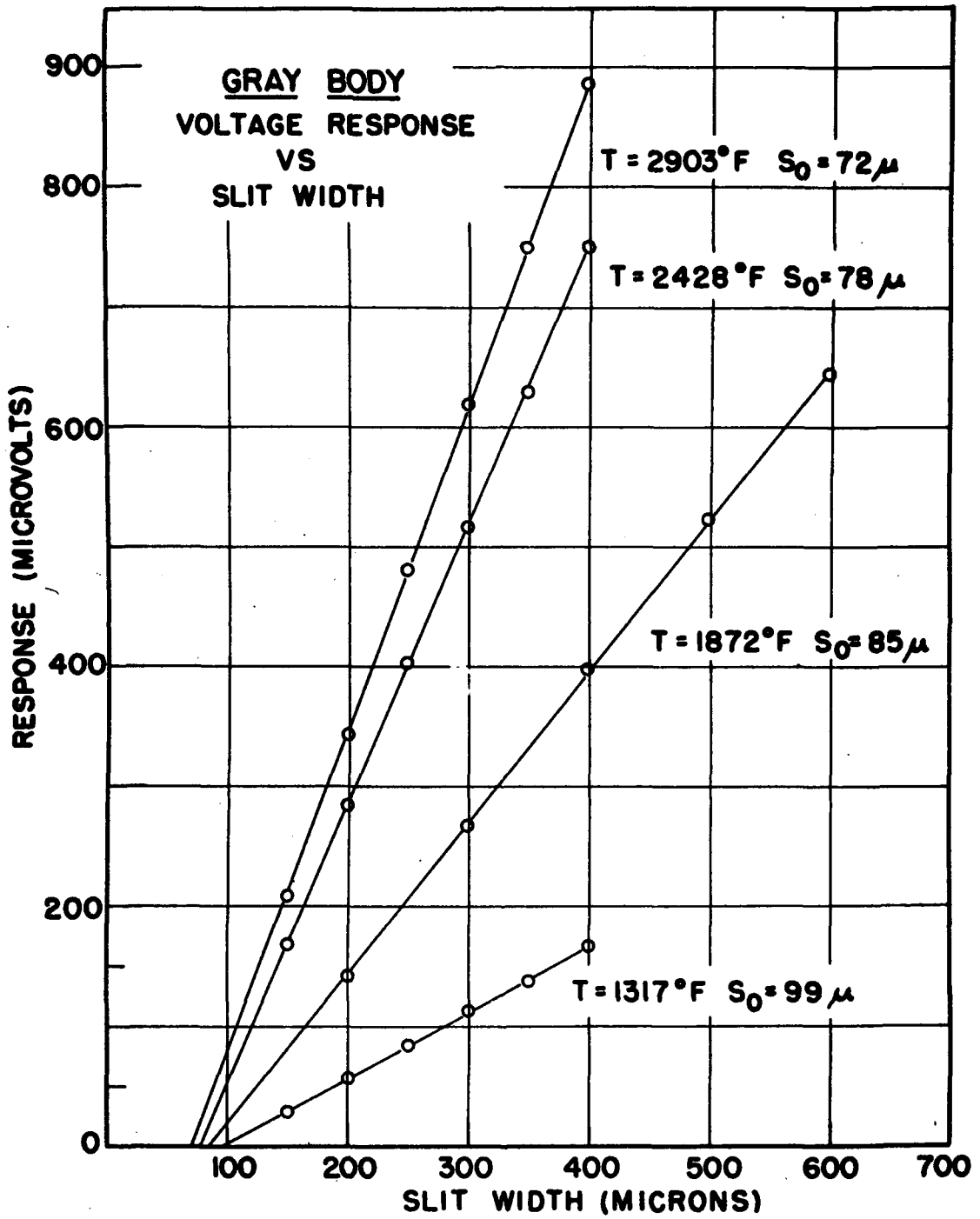

Figure 16. GRAY BODY VOLTAGE RESPONSE VS SLIT WIDTH

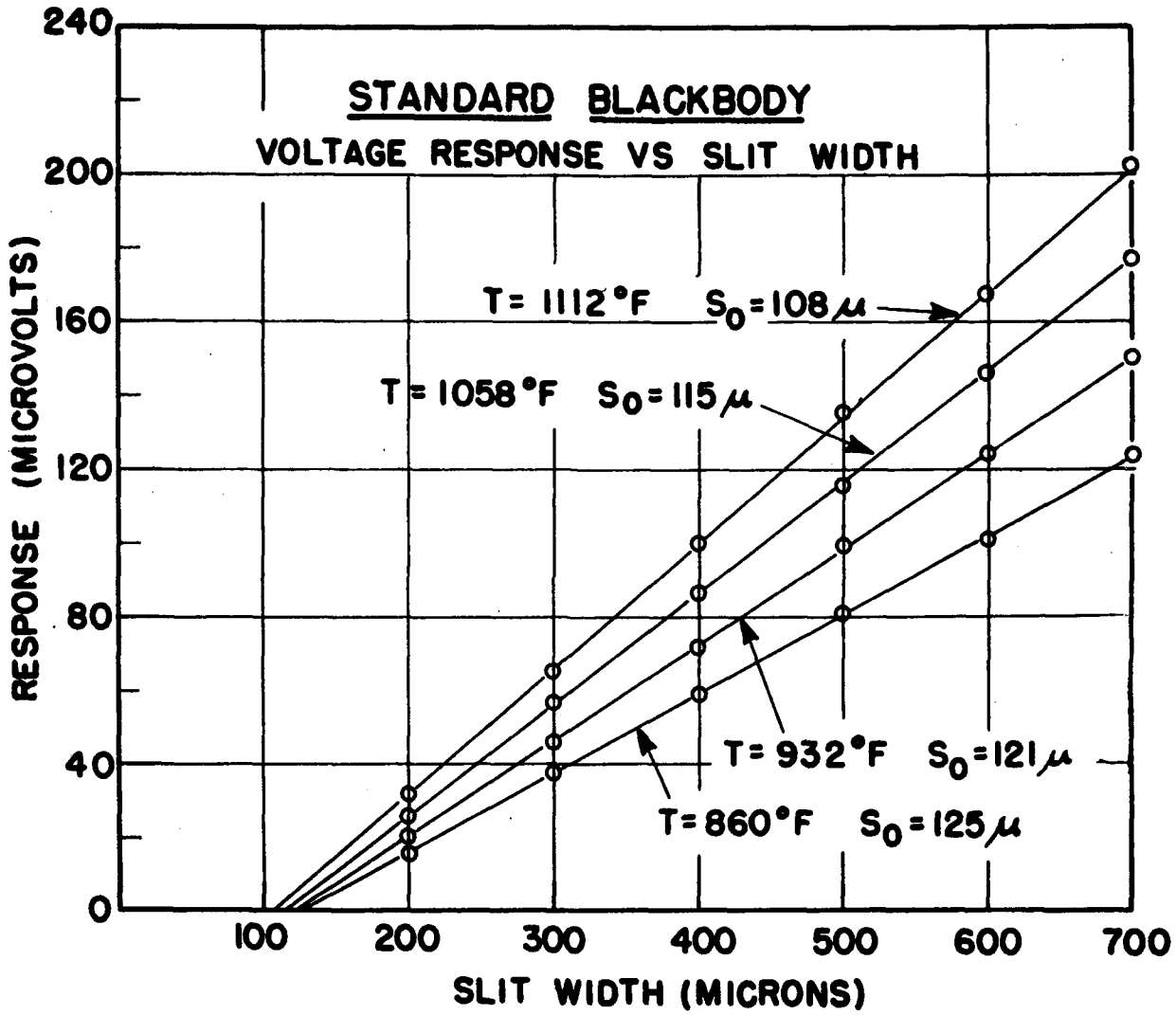

Figure 17. STANDARD BLACKBODY VOLTAGE RESPONSE VS SLIT WIDTH

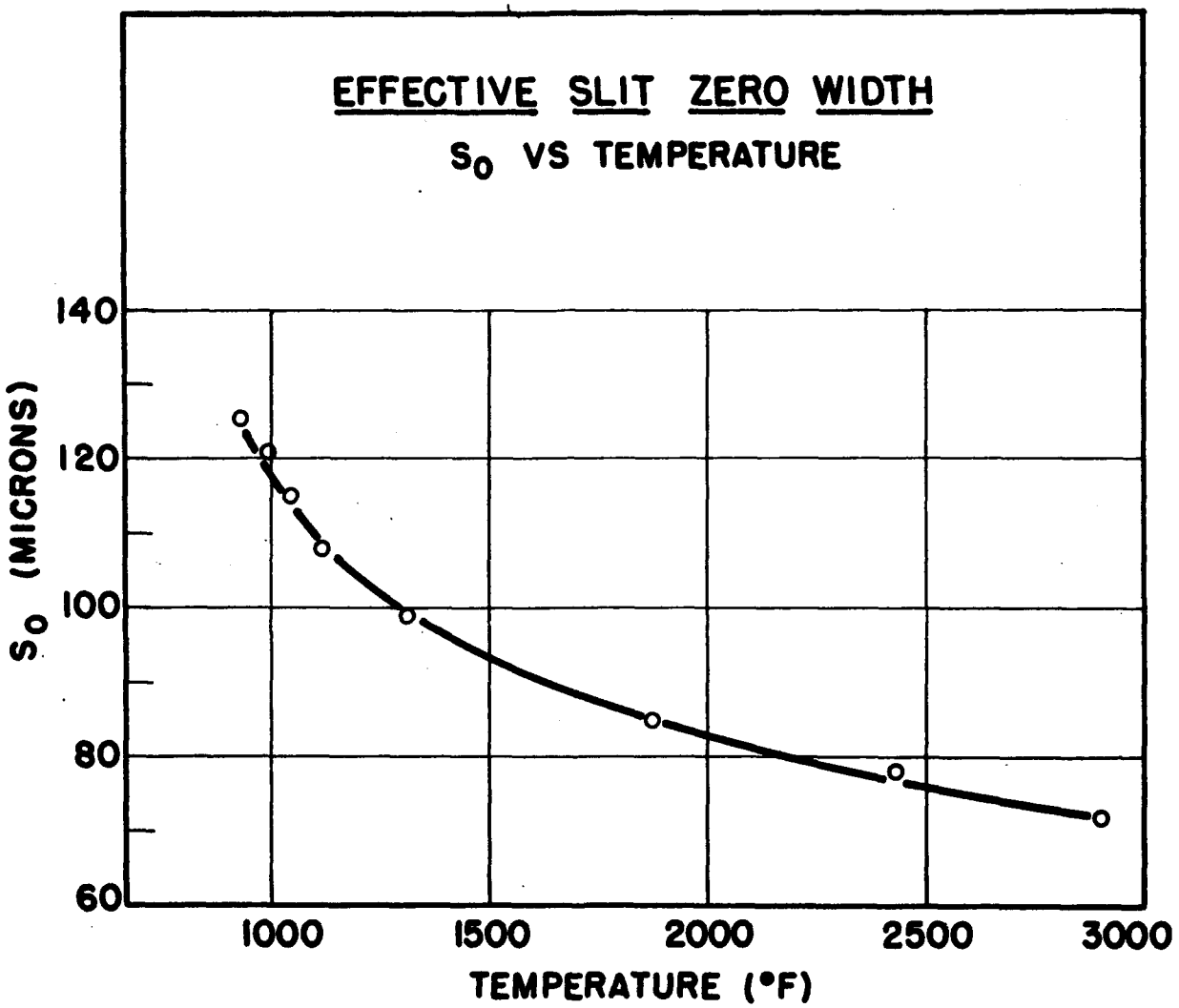

Figure 18. EFFECTIVE SLIT ZERO WIDTH VS TEMPERATURE

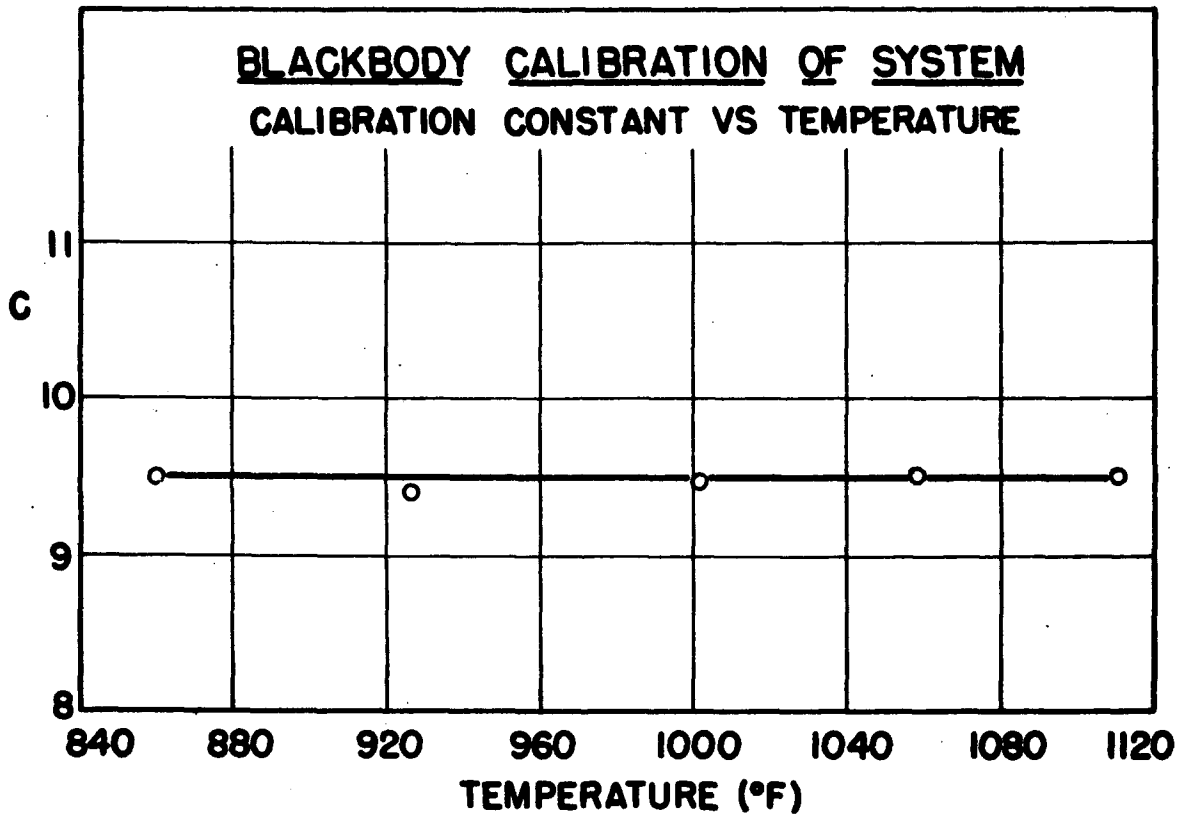

Figure 19. BLACKBODY CALIBRATION OF SYSTEM

2. Test Measurements

The test procedure adopted for this program was designed to provide quantitative information about the total emittance properties of leading edge materials at temperatures up to 3000F. The effects of oxidation on these properties were studied for certain materials. The formal test procedure may be summarized as follows:

a. The total normal emittance of all specimens was measured at selected temperatures in the range 1300-3000F for two complete cycles of heating and cooling from 70F to 3000F. The specimen materials were heated in an atmosphere consisting of 90% argon and 10% hydrogen at a pressure of 78 cm of Hg. The argon-hydrogen mixture was used in place of pure argon to prevent reaction with traces of residual oxygen at the high temperatures.

b. Total angular emittance was then measured for the same specimen at the two temperatures, 1500F and 2500F, at 30°, 45°, and 60° from the outward drawn normal. These measurements were carried out in the argon-hydrogen atmosphere.

c. The coated specimens, Durak MG and W-2, and the siliconized ATJ graphite were heated to 2000F in air and maintained at that temperature for one hour. Following this treatment, steps a and b were repeated. During the course of each run, the specimen temperature was recorded at 5 to 10 minute intervals so that slight temperature changes of the order of 5-10°F could be taken into account.

d. The test procedure outlined in paragraphs a, b, and c was used with one specimen of the molybdenum alloy, one specimen of ATJ graphite, one specimen of siliconized graphite, one specimen of Durak MG - coated molybdenum, and one specimen of W-2 coated molybdenum, as received, and two preoxidized specimens. The angular emittance data for angles other than the normal were recorded for a second specimen of each material.

C. EXPERIMENTAL ACCURACY

The chief sources of error in the emittance measurements are errors in temperature measurement, errors in total emittance measurement and calibration errors. Best estimates of these errors indicate that the reported data (Section D) are accurate to ±5%.

1. Temperature Errors

Two types of errors in temperature measurement were considered: the first of these was error resulting from inexact calibration of the pyrometer; the second was error resulting from non-blackness of the cavity in the sample and attenuation by the NaCl window.

a. Calibration Error

Calibration errors were minimized by frequently recalibrating the pyrometer against a standard tungsten filament lamp. The tungsten lamp used

had been previously calibrated against an NBS black-body standard. In view of the excellent reproducibility of the pyrometer calibration errors here are believed to be less than ±2°F over the entire range.

b. Black-body Cavity

The depth to diameter ratio of the cavity drilled in the specimen was approximately 3:1. If it is assumed that the spectral emittance of the specimen at 0.65 microns (the wavelength of operation of the pyrometer) is ≥0.4, the emissivity of the black-body cavity will be at least 0.92. Temperature errors resulting from such non-blackness will not exceed 10F at 3000F of 2F at 1500F.

c. Attenuation by the NaCl Window

The NaCl window and other optical elements used to direct radiation from the specimen to the pyrometer slightly reduce the intensity of radiation received by the pyrometer. Errors due to such attenuation of the order of 8-10% were avoided by measuring the brightness temperature of a strip filament tungsten lamp first by sighting directly on the lamp and second by sighting on the lamp through the NaCl window and associated optical elements. The temperature correction factor obtained in this manner was in excellent agreement with theory. The correction factor was applied to all temperatures measured with the pyrometer. The NaCl windows were repolished daily to avoid errors due to slight fogging. The temperature correction for the NaCl windows was measured at frequent intervals and was found to be constant.

2. Errors in Total Emissive Power

Errors in total emissive power measurement arise from errors in determining the slit function (Equation 16) and errors in measuring chart deflections or thermocouple voltages. Both sources of error are associated with the noise level and over-all stability of the system. Based on reproducibility considerations, the over-all error in total emittance measurement is believed to be less than ±1%.

3. Calibration Errors

Calibration errors arise from non-blackness of the high temperature black-body standard, temperature fluctuations of the standard, and the errors in determining the slit function and thermocouple voltages cited in (2) above. The black-body standard is reported to be accurate to 1% so that calibration errors should not exceed ±2%.

D. TEST RESULTS

The emittance properties of five potential leading edge materials were determined. Three of the materials were coated -- Durak MG on Mo-Ti alloy, Chromalloy W-2 on Mo-Ti alloy, and siliconized ATJ graphite. Two of the materials, ATJ graphite and the Mo-Ti alloy (Mo + .05% Ti), were uncoated. The effects of oxidation were studied only for the coated materials. The test procedure followed was that outlined in Section B.

1. Mo-Ti Alloy

The total normal emittance of the Mo-Ti alloy is shown in Figure 20 and the total angular emittance at 30°, 45°, and 60° from the normal at 1500F and 2500F in Figure 21. The specimens studied were smooth and flat and exhibited metallic reflection both before and after heating. There was no evidence of oxidation.

The emittance of the Mo-Ti alloy was appreciably lower than that observed for any other material studied, having an average normal emittance of 0.13. The independence of emittance on angle of emission (Figure 21) is attributed to surface roughness (32 microinches rms). This behavior would not be observed for an optically polished specimen.

2. ATJ Graphite

The total normal emittance of ATJ graphite is shown in Figure 22 and the total angular emittance at 30°, 45°, and 60° from the normal at 1400F and 2500F in Figure 23. The specimens studied were smooth and flat both before and after heating.

The ATJ graphite was the blackest material studied, having an average normal emittance of 0.875 that was found to be very nearly independent of temperature. No significant variation of total emittance with angle was observed indicating that the specimens were cosine emitters.

3. Siliconized ATJ Graphite

The siliconized graphite specimens studied were flat but with a rough-textured surface. Total normal emittance data are shown in Figure 24 and angular emittance data in Figure 25 for the as received material.

The angular and normal emittances are nearly identical showing a gradual increase from 0.76 at 1400F to 0.81 at 2400F. With further increase in temperature to 2900F, the emittance decreased to 0.725.

Data for the oxidized specimen are shown in Figure 26. The low temperature portion of the curve (1300-2000F) is similar in shape to that for the as received specimen but about 10% lower. Above 2000F the emittance decreases rapidly, falling to a value of 0.57 at 2950F. This behavior is attributed to the presence of a SiO_2 surface layer formed during oxidation. Above 2000F the SiO_2 layer will become fluid and reduce the effective surface roughness thus leading to the observed decrease in emittance.

4. Chromalloy W-2 on Mo-Ti Alloy

The W-2 coated materials studied were flat and relatively smooth. The visual appearance of the surface as received was not uniform but was mottled, varying in hue from green to brown to gray. After heating the surface coloring was nearly a uniform gray. Some difficulties were experienced with the first W-2 specimens studied. A leak developed in the system and the material at

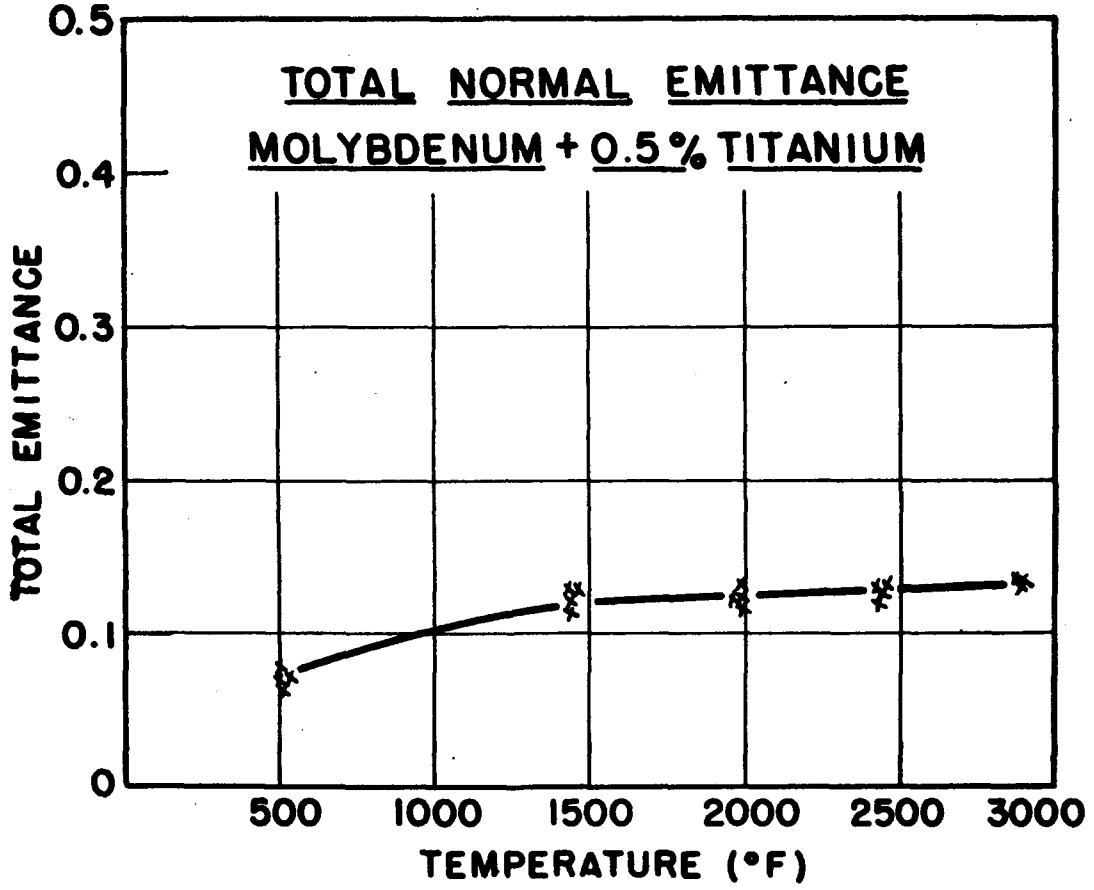

Figure 20. TOTAL NORMAL EMITTANCE OF MOLYBDENUM +0.5% TITANIUM

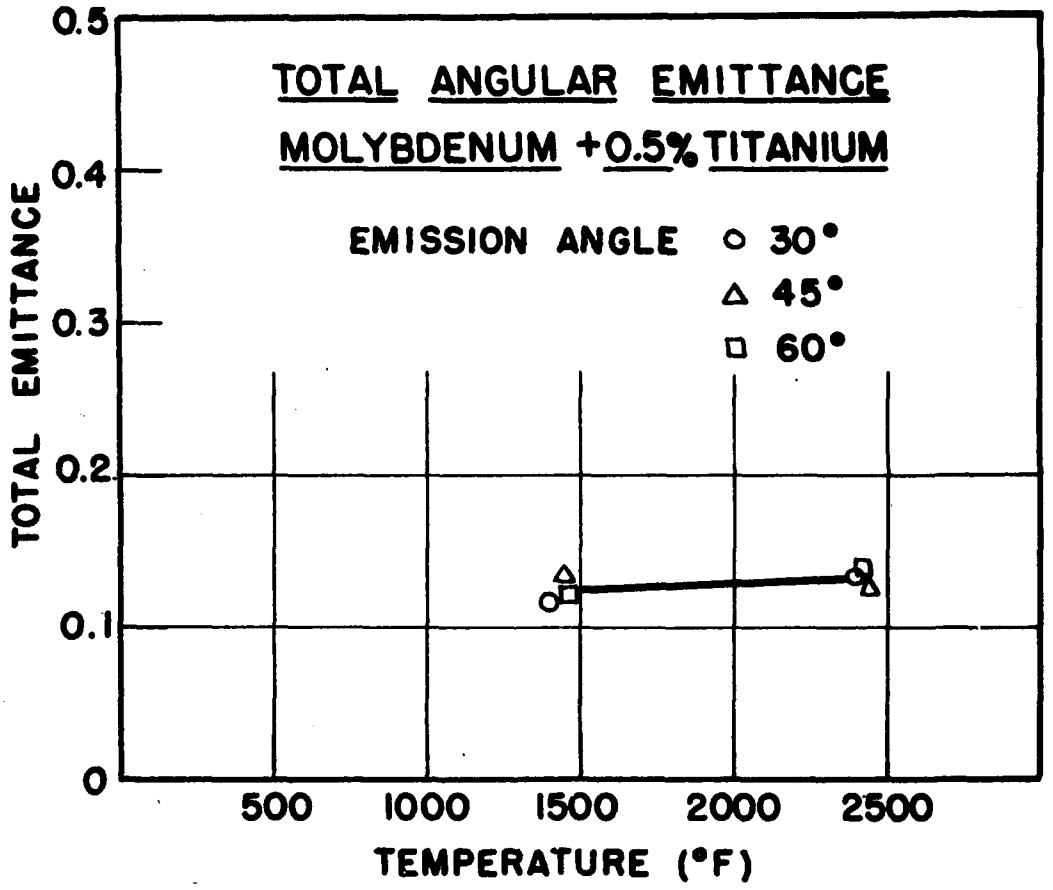

Figure 21. TOTAL ANGULAR EMITTANCE OFMOLYBDENUM +0.5% TITANIUM

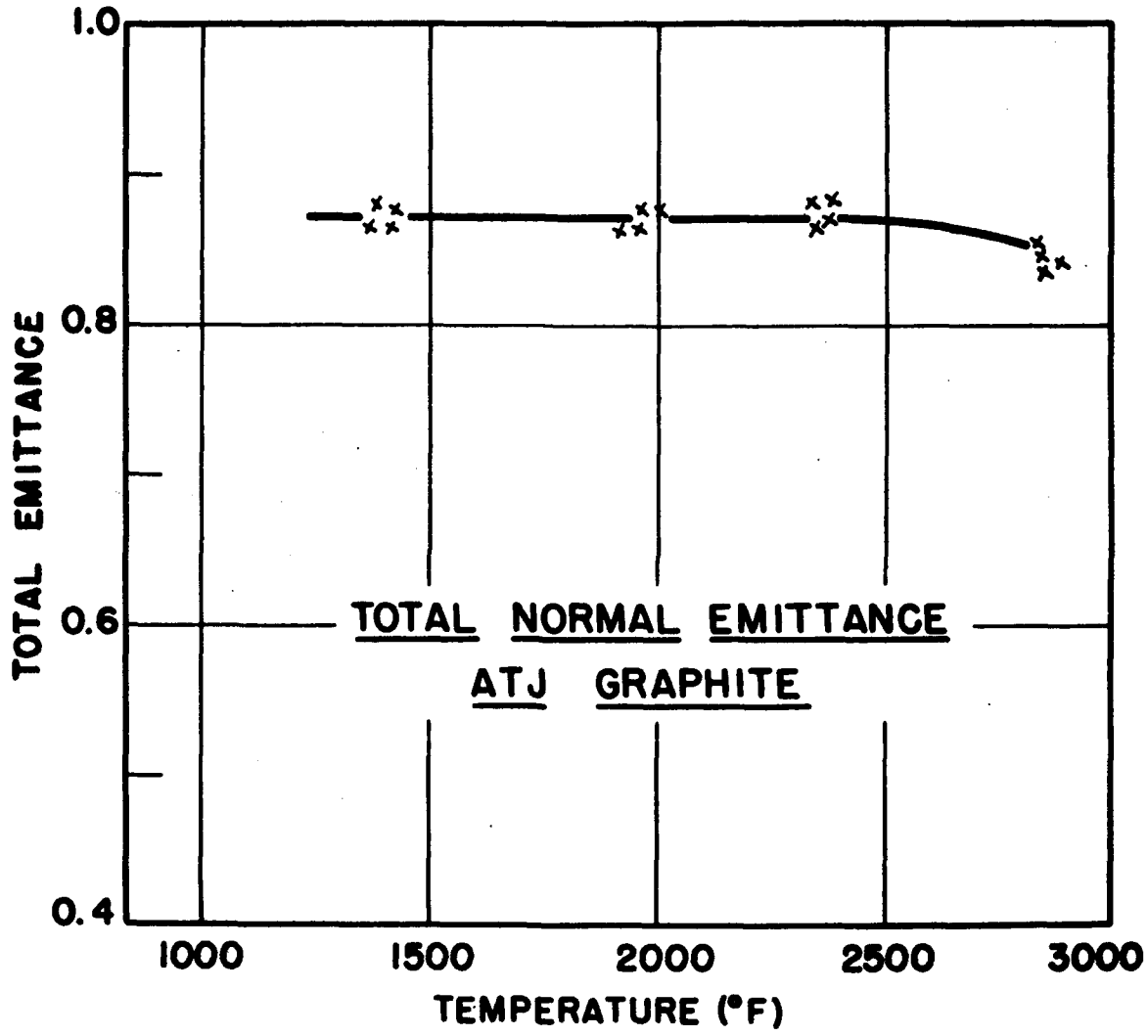

Figure 22. TOTAL NORMAL EMITTANCE OF ATJ GRAPHITE

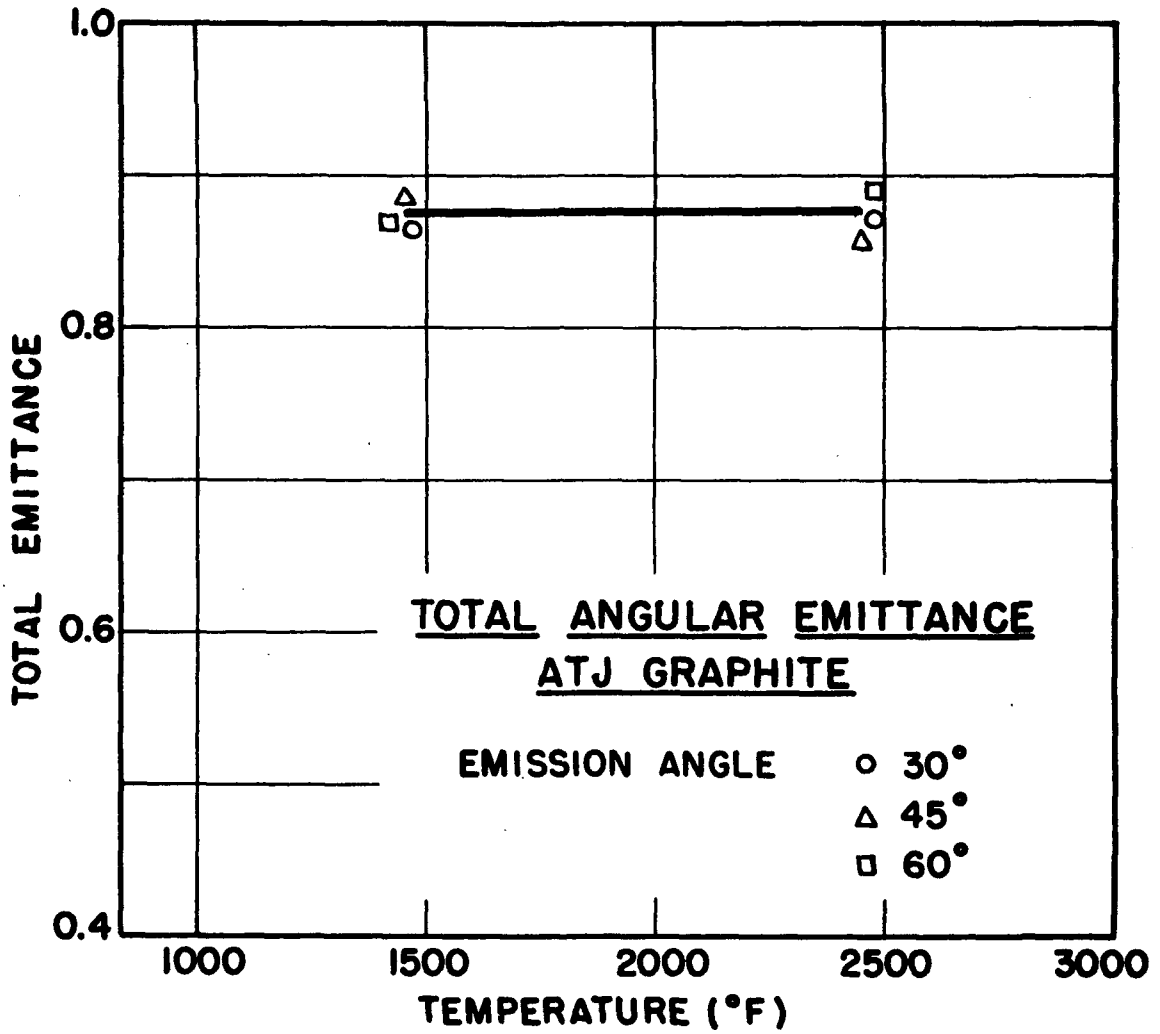

Figure 23. TOTAL ANGULAR EMITTANCE OF ATJ GRAPHITE

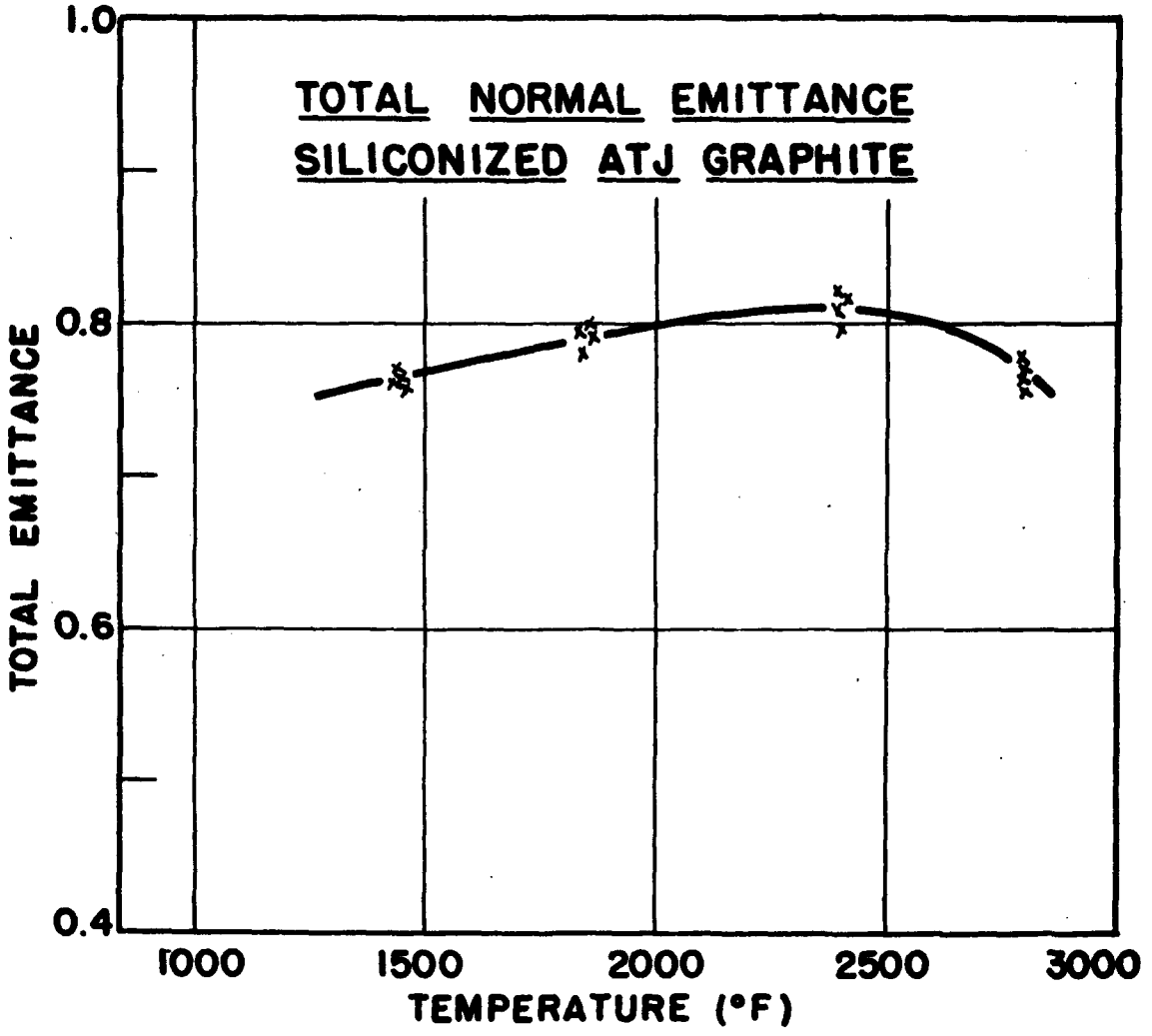

Figure 24. TOTAL NORMAL EMITTANCE OF SILICONIZED ATJ GRAPHITE

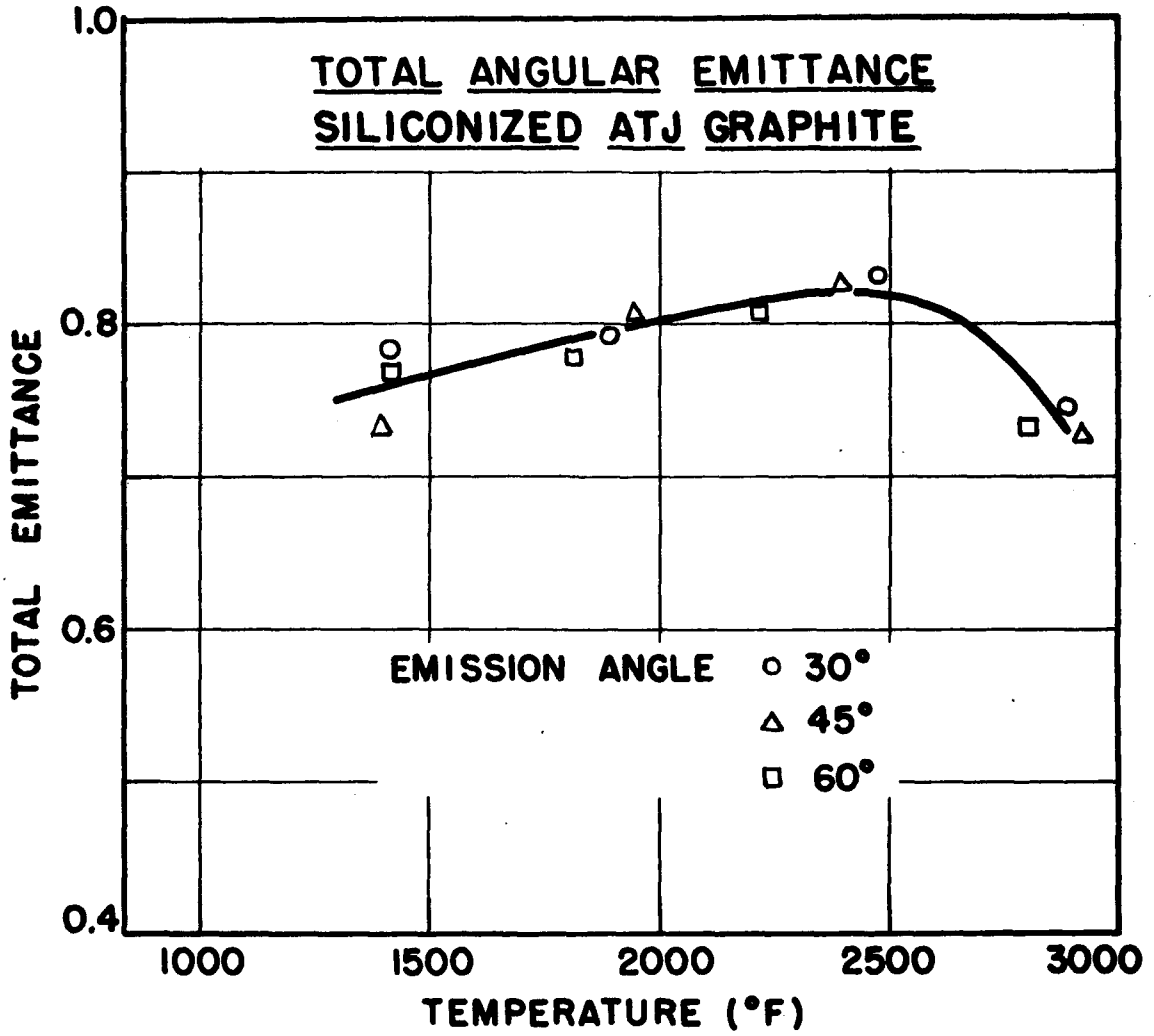

Figure 25. TOTAL ANGULAR EMITTANCE OF SILICONIZED ATJ GRAPHITE

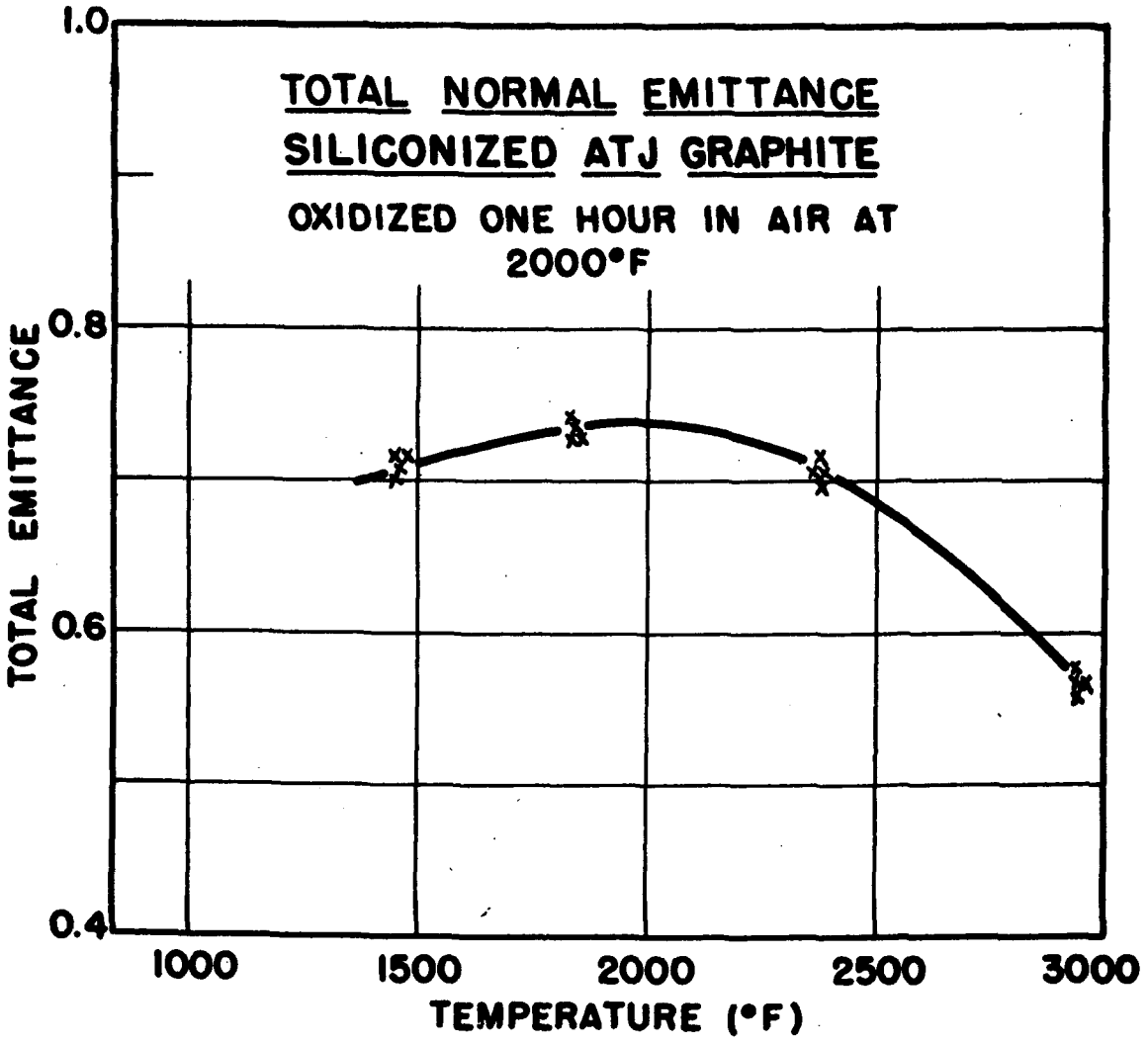

Figure 26. TOTAL NORMAL EMITTANCE OF SILICONIZED ATJ GRAPHITE (OXIDIZED ONE HOUR IN AIR AT 2000°F)

2500F was exposed to air. The coating degenerated badly first developing cracks, then mushroom-shaped protrusions. Finally the Mo-Ti base reacted with oxygen and the sample was destroyed.

After the leak was repaired, a second specimen believed to be identical to the first was studied without difficulty. The total normal emittance data for this material are shown in Figure 27 and the total angular emittance in Figure 28. Here again cosine emission is observed. The emittance increases slowly from a value of 0.60 at 1000F to a maximum of 0.630 at 2330F and then decreases to 0.60 at 2920F.

Normal and angular emittance data for the preoxidized specimens are shown in Figures 29 and 30, respectively. The effects of oxidation on emittance were small except at the highest temperatures.

5. Durak MG on Mo-Ti Alloy

The Durak MG coated specimens were smooth and flat and of a uniform gray color before and after heating in the argon-hydrogen atmosphere and after oxidation. Total normal emittance and total angular emittance for the as received specimen are shown in Figures 31 and 32. The material is a cosine emitter with an average emittance of 0.625 that is essentially independent of temperature up to 2500F. Above 2500F the emittance decreases rapidly.

Data for the preoxidized specimen are shown in Figure 33. Below 2000F the emittance is nearly constant and equal to 0.60. Above 2000F the emittance decreases rather rapidly reaching a value of 0.50 at 2850F.

Although there is no definite information on the chemical composition of the Durak MG coating, it is reported to be similar to the Chromalloy W-2 coating. The decrease in emittance at the higher temperature may be due to the formation and grading of silica.

E. DISCUSSION

The total emittance properties of three coated and two uncoated materials were measured at temperatures ranging from 1300F to 3000F. The materials were heated in a 90% argon, 10% hydrogen atmosphere in order to avoid the effects of oxidation during measurement.

The coated materials were studied both as received from the manufacturer and after oxidation produced by heating in air at 2000F for one hour. Total normal emittance and total angular emittance at 30°, 45°, and 60° from the normal were measured for all five materials. This reported data are believed accurate to ±5%.

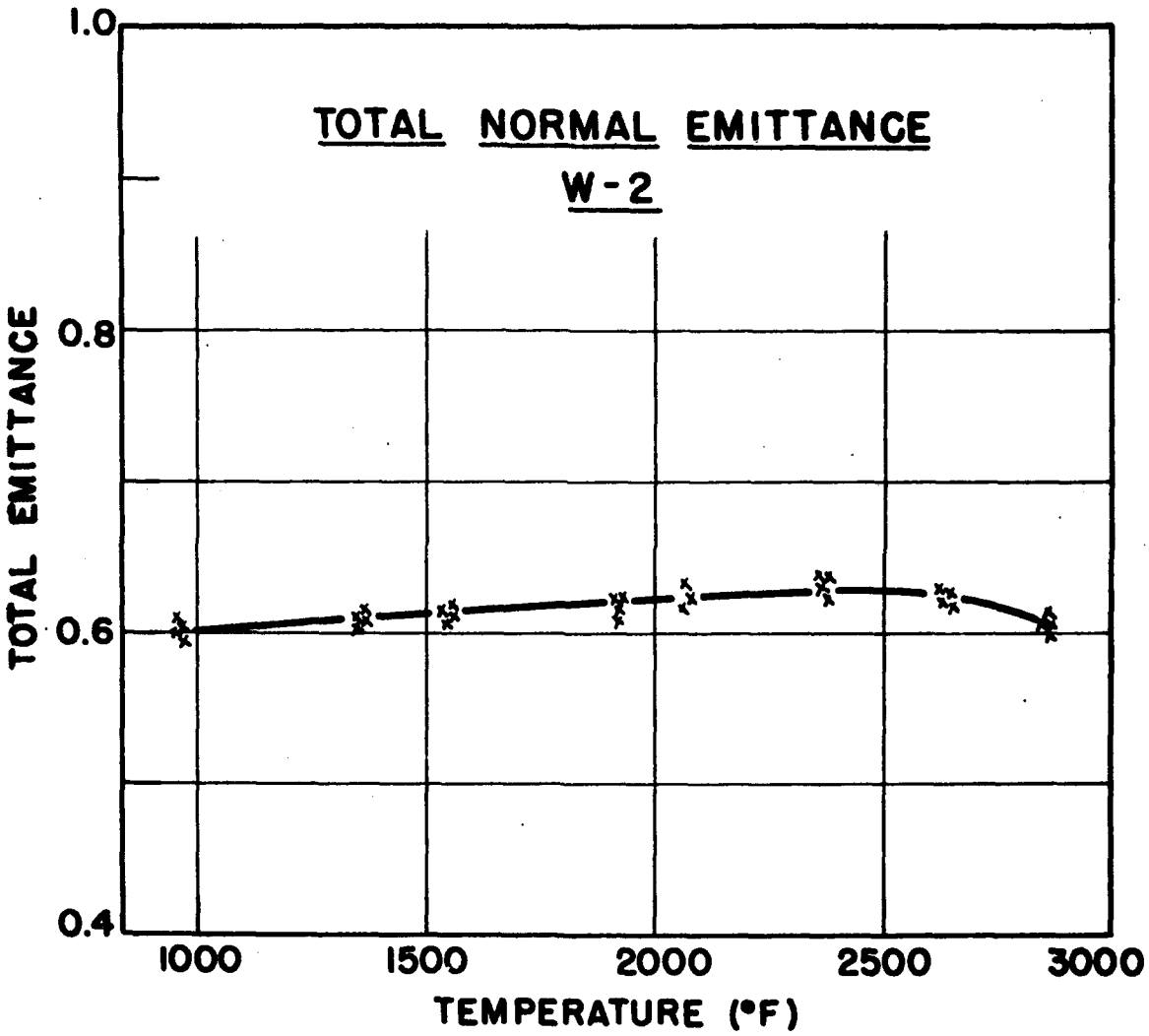

Figure 27. TOTAL NORMAL EMITTANCE OF W-2

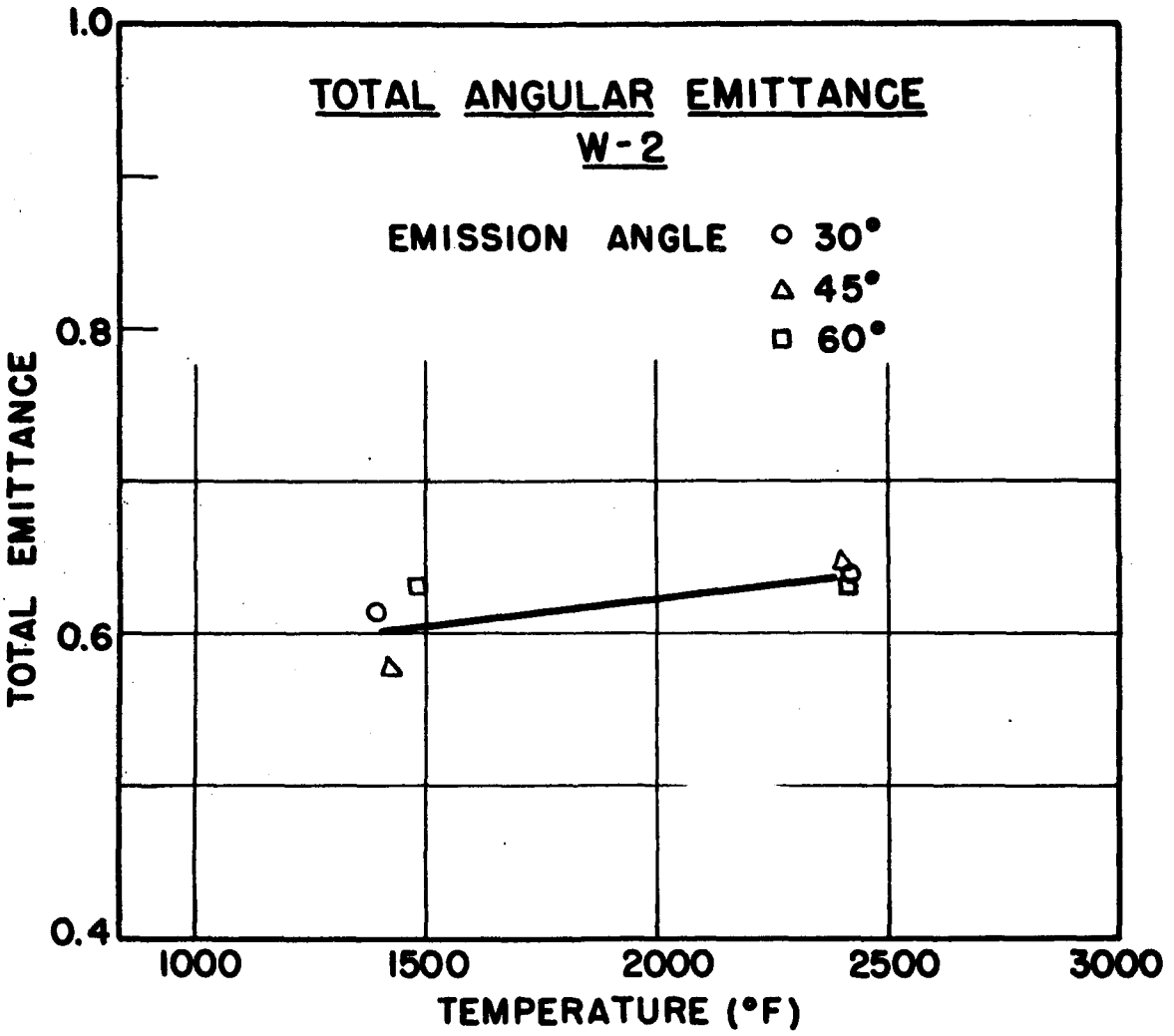

Figure 28. TOTAL ANGULAR EMITTANCE OF W-2

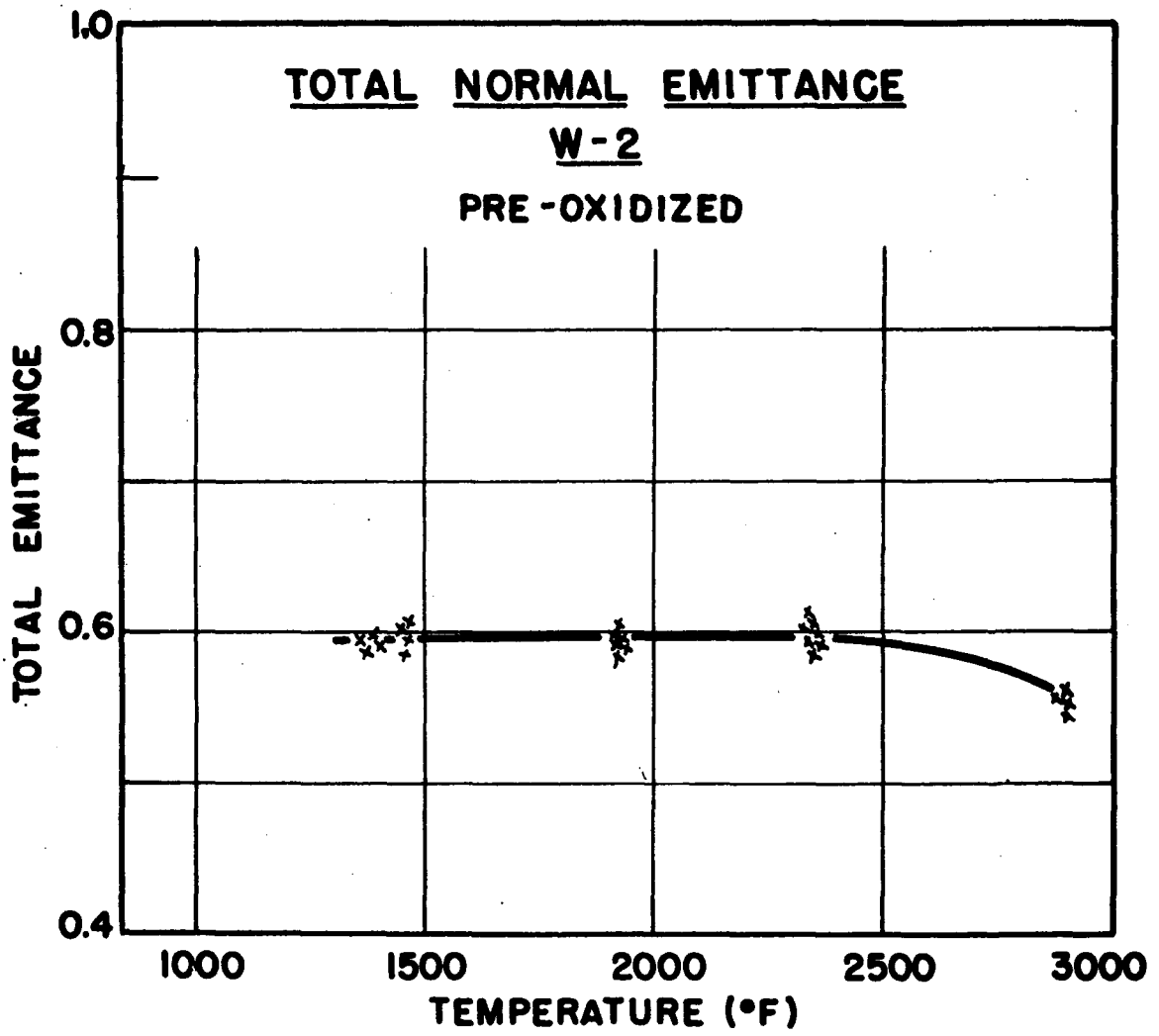

Figure 29. TOTAL NORMAL EMITTANCE OF W-2 (PRE-OXIDIZED)

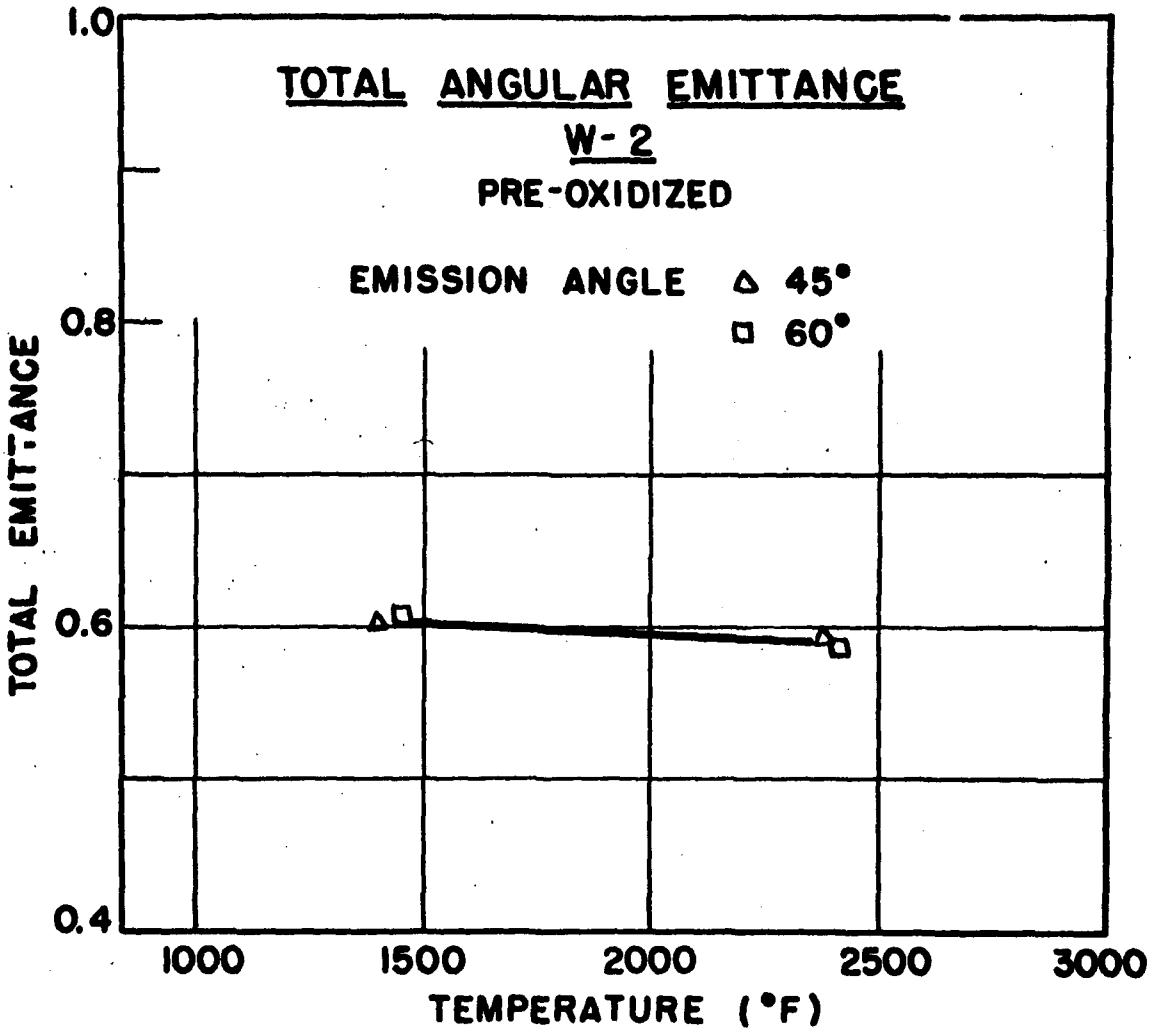

Figure 30. TOTAL ANGULAR EMITTANCE OF W-2 (PRE-OXIDIZED)

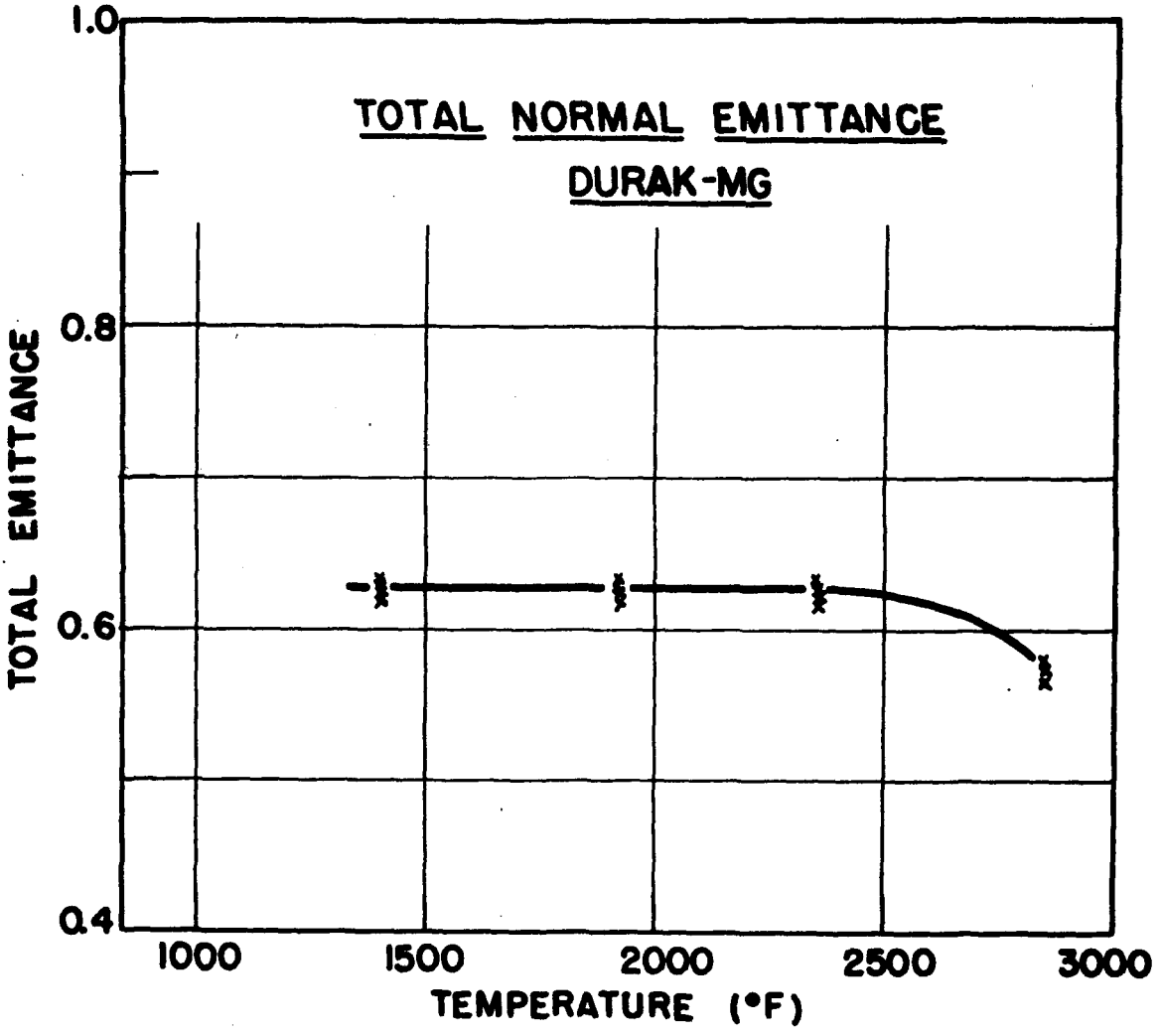

Figure 31. TOTAL NORMAL EMITTANCE OF DURAK-MG

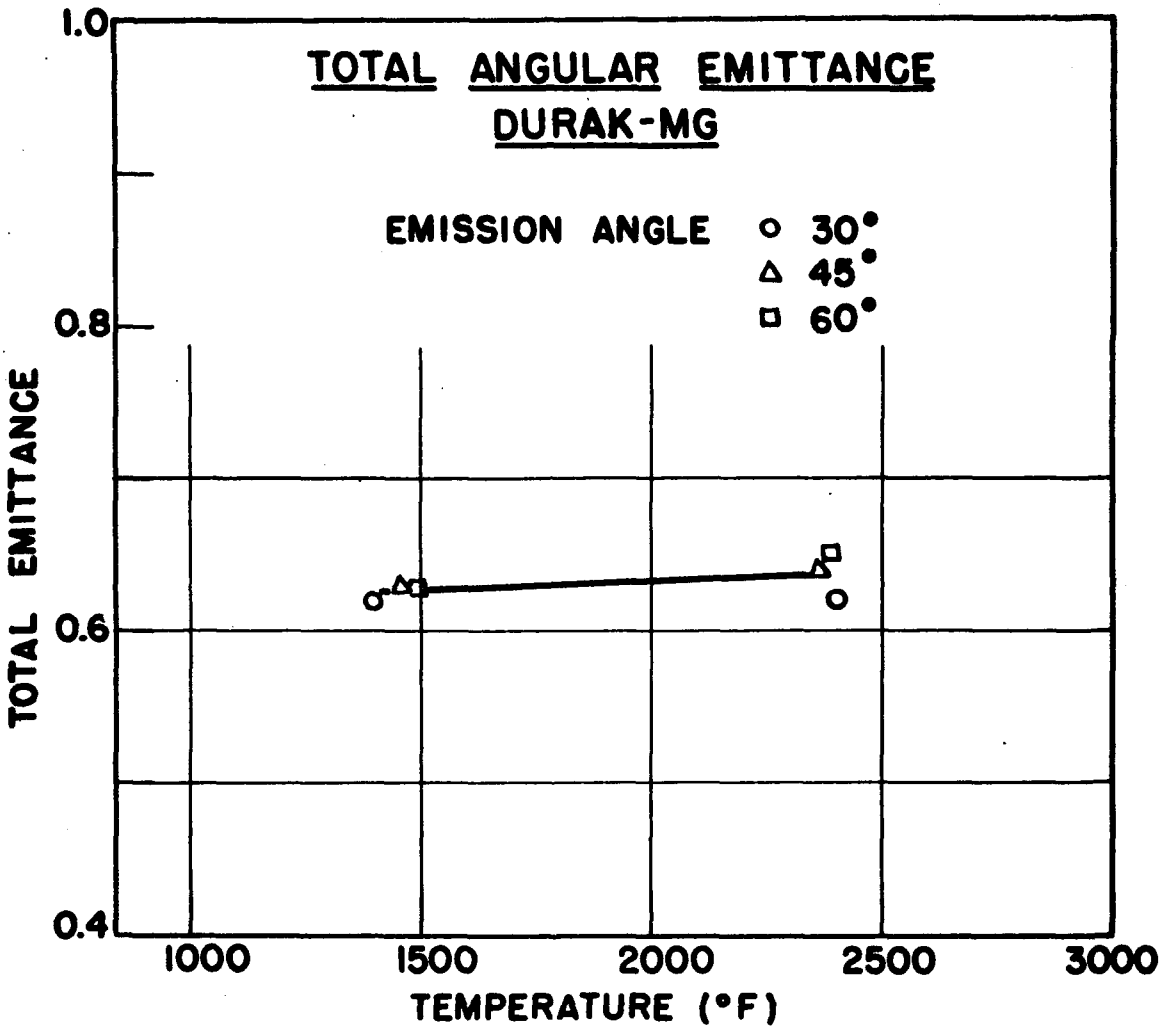

Figure 32. TOTAL ANGULAR EMITTANCE OF DURAK-MG

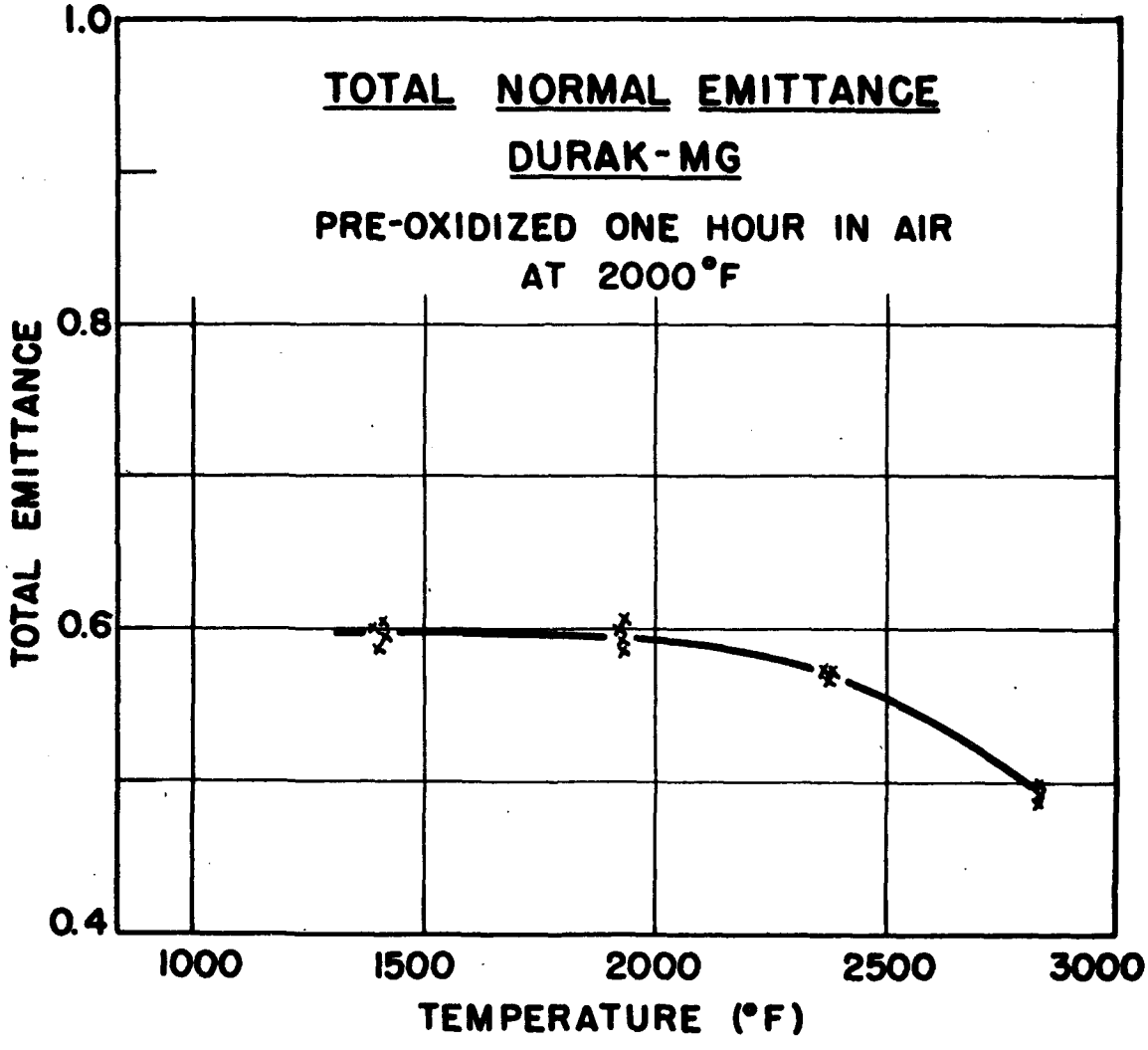

Figure 33. TOTAL NORMAL EMITTANCE OF DURAK-MG
(PRE-OXIDIZED ONE HOUR IN AIR AT 2000°F)

APPENDIX I

DESCRIPTION OF MATERIALS TESTED

The purpose of this appendix is to describe the types of test specimens employed during the evaluations of thermal properties and the materials from which these specimens were fabricated. The fabrication procedures employed were similar to those which would be used for the production of actual leading edge components.

The test specimens used for the evaluation of thermal properties of selected materials are shown in Figures 34, 35 and 36. For the molybdenum alloy the test specimens used for determining thermal conductivity, thermal expansion and specific heat were not coated. Samples used for emissivity measurements included both uncoated and coated specimens. For the graphite material most of the specimens were siliconized. Exceptions to this procedure included thermal emissivity and specific heat test specimens, for which both uncoated and coated specimens were produced.

The 0.5% titanium alloy of molybdenum used for this investigation was recrystallized for 35 minutes at 2900F. This treatment resulted in complete recrystallization with a grain size estimated at approximately ASTM 4. The material used for conductivity, specific heat and emittance specimens was supplied by Universal Cyclops Steel Corporation, Bridgeville, Pennsylvania, while material for the expansion specimens was supplied by General Electric Company, Cleveland, Ohio. The U-C material had the following range of alloying elements: carbon .024 to .031%, titanium .43 to .48%, other .06% maximum of which oxygen, nitrogen and hydrogen constituted a maximum of .005%. The chemistry of G.E. material was not supplied in detail. Nominally this material contained .5% titanium and from .010 to .030% carbon.

The only molybdenum alloy specimens coated were those used for thermal emittance measurements. The W-2 coating was applied by the Chromalloy Corporation of White Plains, New York, and the Durak MG coating was applied by the Chromizing Company of Los Angeles, California. Both processes employ pack deposition techniques wherein parts to be coated are placed in a powdered mixture within a retort. The retort is then sealed and heated to temperatures of approximately 2000F for a period of time. Upon heating the powder generates a gas which reacts with the parts and results in a thin alloyed case having surface finish approximately as smooth as the original base material.

Prior to processing the parts were inspected visually and were lightly etched with nitric acid. In the case of the W-2 processing, a liquid honing operation was also performed. After the cleaning procedure the specimens were again examined and found to be free of defects.

The Durak coating was applied in a single processing run, that is, the full coating thickness, .002 inch, was formed during a single operation. In the W-2 process the desired coating thickness, .004 inch nominal, was applied in a double processing cycle. After the first cycle the parts were unpacked, cleaned, repacked and reprocessed.

After the process was completed the samples were exposed in still air at 2000F to determine continuity of the coating. The exposure time for the Durak specimens was ten minutes while that for the W-2 specimens was one hour. All samples satisfactorily completed this inspection.

The samples coated with Durak MG were processed during December 1959. One of the samples coated with Chromalloy W-2 was coated during August 1959 while the other was coated during October 1959.

Grade ATJ graphite is an extremely fine-grain premium quality graphite. It is molded in blocks 9" x 20" x 24". The maximum grain size is approximately .006 inch and the ash content is approximately .2%. The stock used for the thermal property evaluation specimens was taken from randomly selected material. The quality of the raw material was determined by X-ray inspection of the blocks and bulk density determinations. In order to expedite delivery of these specimens, no further inspections other than dimensional were conducted on these specimens after machining.

The coating applied is essentially a diffusional deposit of silicon carbide-silicon nitride formed by the reaction of silicon containing compounds with the graphite surface. Details of the process are proprietary and cannot be disclosed. During the siliconizing operation the specimens were mounted on knife edges in order to present a maximum of graphite surface to the silicon compounds. Relatively large spacing distances were used between samples. This procedure was found to be necessary as a result of the experience gained during coating of the screening test specimens. The quality of the coated material was checked by weight measurements which were converted to weight gain per unit area. This weight gain could then be compared with the standards established on the basis of previous experience.

Thermal conductivity specimens and thermal expansion specimens of two orientations were fabricated. One set of specimens of each type was machined parallel to grain orientation, while the other set was machined perpendicular to the grain orientation. The ATJ graphite specimens perpendicular to the grain orientation were necessarily short because the maximum dimension of the molded block in that plane is 9 inches. Since the specimens were short they were not tested. All other specimens were machined from stock which was parallel to the grain.

As indicated above, the raw material used was subjected to a rather thorough inspection. After machining, only dimensional inspections were conducted. As a control on the coating process weight gain per unit area was determined. Final inspection of the test specimens consisted of visual examination and dimensional measurements. The more elaborate X-ray inspection procedure and oxidation proof test employed for the mechanical property test specimens was not conducted on the thermal property specimens. These procedures were eliminated in order to expedite delivery.

More complete details of the processing are provided in the appendixes of Volume VI. Weights of the specimens before and after coating as well as coating run numbers are presented in Table XV.

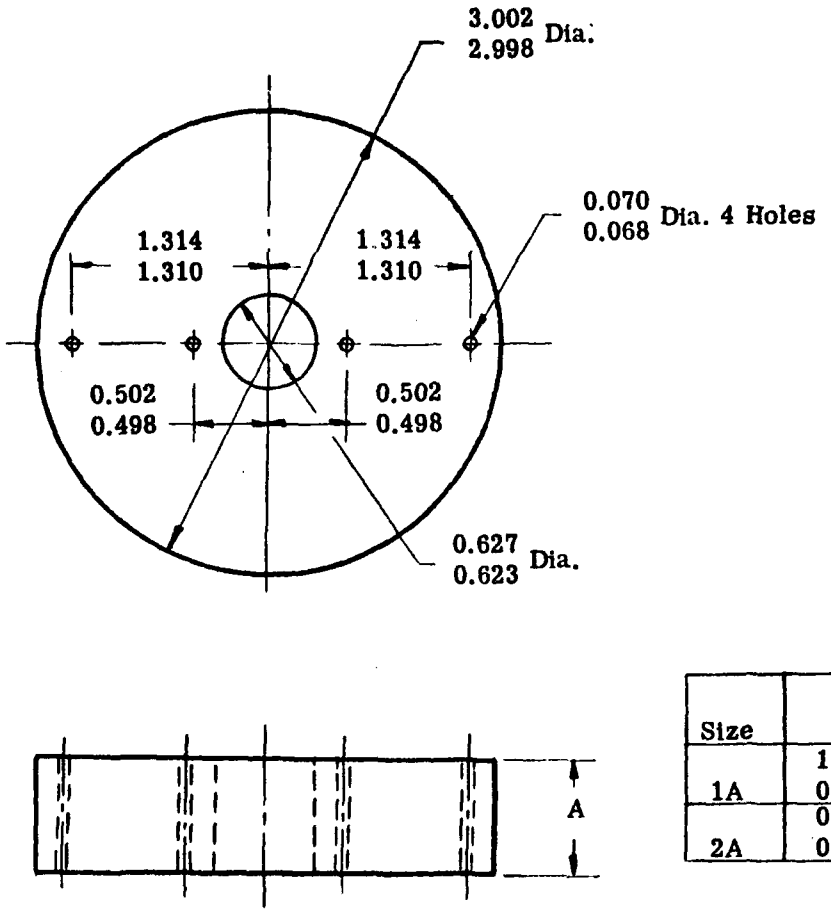

Size	A	No. Set
1A	1.010 0.990	3
2A	0.510 0.490	12

Figure 34. THERMAL CONDUCTIVITY SPECIMEN

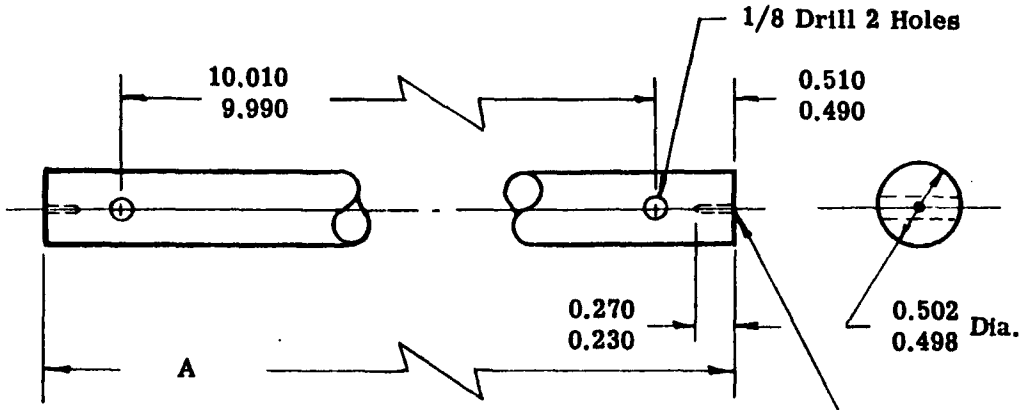

Material	A
Molybdenum Alloy	11.030/10.970
ATJ, Parallel to Grain	11.030/10.970
ATJ, Perpendicular to Grain	9,030/ 8.970

Thermal Expansion Specimen

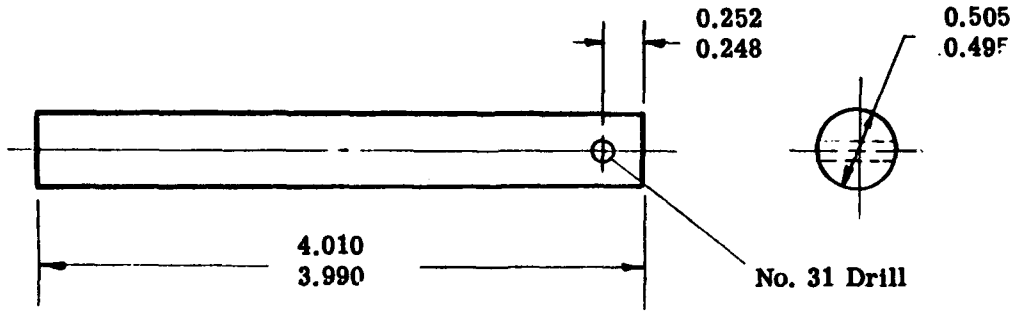

Specific Heat Specimen

Figure 35. THERMAL EXPANSION AND SPECIFIC HEAT SPECIMENS

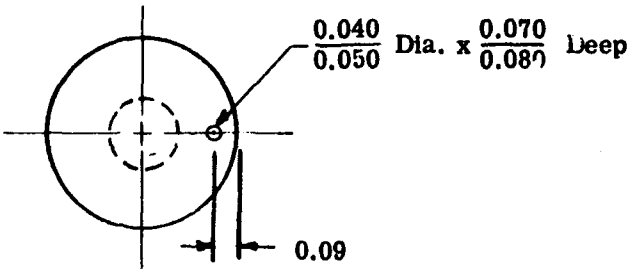

NOTE: All dimensions ±0.010 unless noted. Break all edges 0.02 to 0.03
63 √ unless noted.

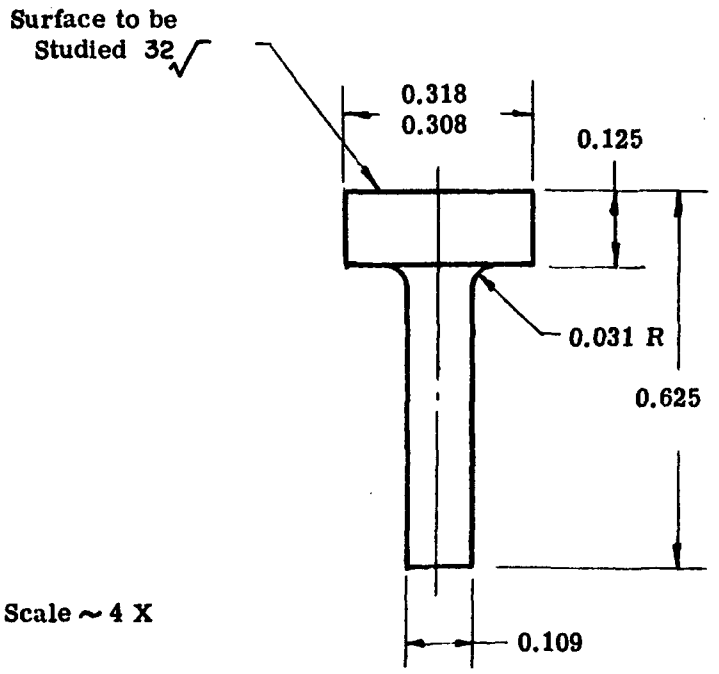

Figure 36. THERMAL EMISSIVITY SPECIMEN

TABLE XV

PROCESSING HISTORY OF DELIVERED GRAPHITE SPECIMENS

Specimen Type No.	Grams Weight Change During Coating: Before	After	Pickup	Coating Run
C-3b Thermal Expansion Specimen				
B-1-9 in. **	48.14	52.52	4.38	G-18
4-9 in.	48.11	52.00	3.89	G-18
3-4-11 in.	58.35	61.13	2.78	G-13
5-11 in.	60.89	63.32	2.43	G-13
Thermal Conductivity Specimen C-4a Size I				
C-2*	192.71	202.30	9.59	G-13
3*	191.11	204.16	13.05	G-13
B-1 T - L**	192.97	197.65	4.68	H-71E-H69W
2 T - L**	193.96	198.49	4.52	H-71E-H69W
3 T - L**	200.17	202.89	2.74	H-71E-H69W
4 T - L**	192.59	199.39	6.87	H-66E
5 T - L**	197.43	199.76	2.35	H-66E
1 T - T	197.65	200.50	5.58	H-66E
2 T - T	198.86	199.36	3.11	H-66E
C-4a Size Ia				
D-6*	192.28	201.09	8.81	G-13
7*	192.78	200.23	7.45	G-13
C-1 T - T	194.31	200.72	7.02	H-67W-H73E
4 T - T	194.50	201.34	7.42	H-67W-H73E
11 T - T	196.94	202.00	5.64	H-67W-H73E
12 T - T	196.47	203.81	7.89	H-67W-H73E
13 T - T	191.62	197.97	6.87	H-69W-H73E
16 T - T	200.39	206.85	6.46	H-89E
17 T - T	200.96	206.97	6.01	H-89E
1 T - L	192.92	197.51	4.59	H-66E
2 T - L	193.15	197.88	4.73	H-66E-H73E
3 T - L	200.30	202.41	2.31	H-66E-H73E
4 T - L	192.92	199.85	6.93	H-66E-H73E
5 T - L	197.19	201.89	4.70	H-66E-H73E
10 T - L	193.40	199.68	6.28	H-66E-H73E

Specimen Type No.	Grams Weight Change During Coating: Before	After	Pickup	Coating Run
C-4a Size 2 Thermal Conductivity Specimen				
1*	93.28	99.52	6.24	G-13
3*	92.63	99.48	6.85	G-13
4*	95.14	99.87	4.73	G-13
6*	92.86	103.29	10.43	G-13
10*	93.42	99.22	5.80	G-13
11*	93.20	98.01	4.81	G-13
12*	92.97	98.73	5.76	G-13
15*	93.31	98.29	4.98	G-13
19*	96.61	101.82	5.21	G-13
1 T - T	96.22	100.85	4.63	H-69W and H-66E
2 T - T	94.42	100.33	5.81	H-69W and H-66E
3 T - T	95.84	100.41	4.57	H-69W and H-66E
4 T - T	95.21	99.93	4.72	H-73E and H-66E
5 T - T	86.39	104.03	17.64	H-69W and H-66E
6 T - T	94.39	98.42	4.03	H-69W and H-66E
7 T - T	95.22	101.35	6.13	H-66E
8 T - T	95.25	100.25	5.00	H-66E
9 T - T	94.76	100.45	5.69	H-66E
10 T - T	98.60	101.35	2.75	H-66E
11 T - T	95.78	101.10	5.32	H-66E
12 T - T	95.38	100.46	5.08	H-66E
21 T - T	99.20	101.58	2.38	H-73E and H-69W
23 T - T	100.20	101.85	1.65	H-73E and H-69W
24 T - T	100.09	103.04	2.95	H-73E and H-69W
1 T - L	94.41	100.64	6.23	H-73E and H-67W
2 T - L	91.48	100.00	8.52	H-73E and H-67W
4 T - L	94.95	102.27	8.32	H-82W
5 T - L	94.39	102.78	8.39	H-73E and H-82W
7 T - L	95.20	102.78	7.58	H-73E and H-82W
8 T - L	93.82	102.71	8.89	H-73E and H-82W
11 T - L	92.22	99.18	6.96	H-73E and H-82W
12 T - L	94.34	102.11	7.77	H-73E and H-82W
25 T - L	98.33	101.89	3.56	H-89E
26 T - L	99.28	102.60	3.32	H-89E
27 T - L	99.60	101.65	2.05	H-89E
28 T - L	98.33	101.39	3.06	H-89E
29 T - L	98.40	101.14	2.74	H-89E
30 T - L	98.71	102.60	3.89	H-89E
31 T - L	98.99	102.13	3.14	H-89E

TABLE XV (continued)

PROCESSING HISTORY OF DELIVERED
GRAPHITE SPECIMENS

C-4a Size 2a
Thermal Conductivity Specimen

Specimen Type No.		Grams Weight Change During Coating Before	After	Pickup	Coating Run
5*		93.66	97.86	4.20	G-13
7*		93.43	98.14	4.71	G-13
11*		93.80	97.99	4.19	G-13
14*		93.48	97.86	4.38	G-13
16*		93.55	101.83	8.28	G-13
17*		94.15	99.51	5.36	G-13
18*		94.18	100.28	6.10	G-13
20*		94.98	100.36	5.38	G-13
22*		94.00	99.61	5.61	G-13
1	T - T	94.82	99.35	4.53	H-66E
2	T - T	92.58	102.09	9.51	H-66E
3	T - T	90.13	100.87	10.74	H-66E
4	T - T	98.48	102.46	3.98	H-66E
5	T - T	96.18	101.12	4.94	H-66E
6	T - T	94.42	100.44	6.02	H-66E
7	T - T	97.00	102.02	5.02	H-66E
8	T - T	94.39	100.46	6.07	H-66E
11	T - T	98.18	99.69	1.51	H-71E
12	T - T	95.80	98.03	2.23	H-71E
17	T - T	97.94	101.61	3.67	H-66E
18	T - T	89.68	103.01	13.33	H-66E
21	T - T	94.88	99.33	4.45	H-66E
22	T - T	96.43	99.38	2.95	H-66E
23	T - T	93.63	98.61	4.98	H-66E
25	T - T	94.35	99.02	4.67	H-66E
39	T - T	95.01	100.26	5.25	H-66E
48	T - T	97.90	102.08	4.18	H-89E
49	T - T	97.70	104.04	6.34	H-89E
50	T - T	97.22	101.09	3.87	H-89E
51	T - T	97.00	101.05	4.05	H-89E
52	T - T	96.70	101.20	4.50	H-89E
53	T - T	97.62	101.68	4.06	H-89E
54	T - T	97.76	101.40	3.64	H-89E
55	T - T	97.62	102.18	4.56	H-89E
56	T - T	97.62	102.14	4.52	H-89E
57	T - T	97.55	102.88	5.33	H-89E
2	T - L	97.43	101.45	4.02	H-71E and H-67W
3	T - L	94.62	100.00	5.38	H-71E and H-67W
4	T - L	97.26	100.90	3.64	H-71E and H-67W
5	T - L	97.40	101.49	4.09	H-71E and H-67W
6	T - L	98.01	101.94	3.93	H-71E and H-67W
7	T - L	94.86	100.19	5.33	H-71E and H-69W
9	T - L	96.02	100.87	4.85	H-71E and H-69W
10	T - L	96.48	101.11	4.63	H-71E and H-69W
11	T - L	95.41	101.85	6.44	H-71E and H-69W
12	T - L	94.67	98.90	4.23	H-71E and H-67W
14	T - L	96.03	102.08	6.05	H-71E and H-69W
15	T - L	94.45	97.79	3.34	H-71E and H-67W
23	T - L	94.63	103.59	8.96	H-71E and H-69W
28	T - L	94.70	98.58	3.88	H-71E and H-69W
29	T - L	97.32	101.35	4.03	H-71E and H-67W
30	T - L	94.86	98.81	3.95	H-71E and H-69W
31	T - L	95.90	100.30	4.40	H-71E and H-67W
32	T - L	94.93	99.40	4.47	H-71E and H-67W
33	T - L	94.80	101.02	6.22	H-71E and H-67W
34	T - L	94.99	99.84	4.85	H-71E and H-67W
35	T - L	98.38	102.26	3.88	H-71E and H-67W
39	T - L	95.25	98.90	3.65	H-71E and H-69W
42	T - L	94.93	98.58	3.65	H-71E and H-69W
43	T - L	95.75	99.18	3.43	H-71E and H-69W

C-4c
Specific Heat Specimen

Specimen Type No.		Grams Weight Change During Coating Before	After	Pickup	Coating Run
5		11.89	13.10	1.21	G-13
6		11.88	13.05	1.17	G-13
6	T - L	11.81	12.91	1.10	H-58W
8	T - L	11.82	12.44	0.62	H-58W
9	T - L	11.87	12.50	0.63	H-58W
10	T - L	11.82	12.39	0.57	H-58W
11	T - L	11.87	12.32	0.45	H-58W
12	T - L	11.84	12.34	0.50	H-58W

TABLE XV (continued)

PROCESSING HISTORY OF DELIVERED GRAPHITE SPECIMENS

C-5a Emissivity Specimen

Specimen Type No.		Grams Weight Change During Coating Before	After	Pickup	Coating Run
1		0.3324	0.4472	0.1148	G-13
2		0.3330	0.4514	0.1184	G-13
6	T - L	0.3451	0.3824	0.0373	H-58W
7	T - L	0.3472	0.3884	0.0412	H-58W

C-5b Emissivity Specimen

Specimen Type No.		Grams Weight Change During Coating Before	After	Pickup	Coating Run
1		81.96	88.06	6.10	G-13
2		84.80	88.47	3.67	G-13
2	T - L	82.22	82.90	0.68	H-58W
3	T - L	81.89	83.17	1.28	H-58W
4	T - L	81.66	83.21	1.55	H-58W
6	T - L	82.05	82.72	0.67	H-58W

* Orientation unknown, not used for tests.

** T - L: Thickness of specimen is parallel to 24 in. dimension of graphite block.

T - T: Thickness of specimen is parallel to 9 in. dimension of graphite block.

9 in.: Length of specimen is parallel to 9 in. dimension of graphite block.

11 in.: Length of specimen is parallel to 24 in. dimension of graphite block.

Block size is 9 in. x 20 in. x 24 in. with pressure applied to the 20 in. x 24 in. face.

AD
BELL AIRCRAFT CORPORATION, Buffalo, N.Y.
INVESTIGATION OF FEASIBILITY OF UTILIZING AVAILABLE HEAT RESISTANT MATERIALS FOR HYPERSONIC LEADING EDGE APPLICATIONS, Volume IV Thermal Properties of Molybdenum Alloy and Graphite by I.B. Fieldhouse, J.I. Lang, Armour Research Foundation and H.H. Blau, Jr., Arthur D. Little, Inc. July 1960 (WADC TR 59-744, Volume IV) (Contract 33(616)-6034)
Unclassified Report

The purpose of this contract was to investigate the feasibility of utilizing available heat resistant materials in the fabrication of leading edges for hypersonic boost-glide vehicles. This particular volume presents the results of measurements of the thermal

(over)

UNCLASSIFIED

AD
BELL AIRCRAFT CORPORATION, Buffalo, N.Y.
INVESTIGATION OF FEASIBILITY OF UTILIZING AVAILABLE HEAT RESISTANT MATERIALS FOR HYPERSONIC LEADING EDGE APPLICATIONS, Volume IV Thermal Properties of Molybdenum Alloy and Graphite by I.B. Fieldhouse, J.I. Lang, Armour Research Foundation and H.H. Blau, Jr., Arthur D. Little, Inc. July 1960 (WADC TR 59-744, Volume IV) (Contract 33(616)-6034)
Unclassified Report

The purpose of this contract was to investigate the feasibility of utilizing available heat resistant materials in the fabrication of leading edges for hypersonic boost-glide vehicles. This particular volume presents the results of measurements of the thermal

(over)

UNCLASSIFIED

UNCLASSIFIED

AD
conductivity, specific heat, linear thermal expansion, and emittance of a 0.5% titanium alloy of molybdenum, and of siliconized ATJ graphite as a function of temperature. Emittance measurements were made on coated and uncoated materials.

UNCLASSIFIED

UNCLASSIFIED